THE SYNTHESIS OF *N*-HYDROXYOXINDOLE-BASED PHOTOACTIVATABLE FLUOROPHORES AND ITS APPLICATION FOR BIOIMAGING

By

AN YU

A thesis submitted to the

Graduate School-New Brunswick

Rutgers, The State University of New Jersey

In partial fulfillment of the requirements

For the degree of

Master of Science

Graduate Program in Chemistry and Chemical Biology

Written under the direction of

Ki-Bum Lee

And approved by

_____

_____

_____

New Brunswick, New Jersey

January, 2016

ABSTRACT OF THE THESIS

The Synthesis of *N*-Hydroxyoxindole-Based Photoactivatable Fluorophores and Its Application for Bioimaging

by AN YU

Thesis Director:

Professor Ki-Bum Lee

Photoactivatable fluorophores are essential tools for investigating the dynamic molecular interactions within biological systems with high spatiotemporal resolution. Herein, we report a class of photoactivatable fluorescent *N*-hydroxyoxindoles formed *via* intramolecular photocyclization of *o*-nitrophenyl ethanol (ONPE). These substituted oxindole fluorophores are substantially small in size, show ultra-high fluorescence enhancement (up to 800-fold) for photoactivation and exceptional biocompatibility, generating only water molecules as the photolytic side-product. Structure-activity relationship analysis revealed a strong correlation between the fluorescent properties of these fluorophores and the substituent groups, which can potentially serve as a guideline for designing fluorescent probes with desired photophysical properties. As a proof-of-concept study, a substituted ONPE with uncaging wavelength of 365-405 nm and excitation/emission at 515 and 620 nm respectively was developed. We then demonstrated the capability of this fluorescent probe in the selective imaging of human neural stem cells and HeLa cells. The rapid photoactivation capability of this probe, coupled with its

high biocompatibility allowed for spatially-selective cell labeling with ignorable effect on the cell viability.

Acknowledgements

First and foremost, I would like to give my sincere thanks to my advisor Prof. Ki-Bum Lee for his continuous supports of my M.S. study and genuine advises to my researches. His meticulous attitude towards science sets a rather high standard to everyone in his lab. I'm no exception. He's not only a wise and helpful research advisor who gave me a lot of instructions when I meet difficulties, but also a great mentor who always inspires and supports me.

I also would like to extend my gratitude to my other committee members, Prof. Ralf Warmuth and Prof. Eric Garfunkel for their critical comments and valuable suggestions on my OFRP, IFRP and thesis. Also I will never forget the help these three aforementioned professors gave concerning my next stage studies.

I would like to thank everyone in KBLee Group who plays an unforgettable part in my two year studies here at Rutgers. As a senior in both my undergraduate school Wuhan University and here, Yixiao Zhang is the first guy I meet in this university. It was he who introduced the whole department in our first meeting. He sets up the example of how to be a helpful senior. Next, I would like to thank Letao Yang for the help he gave to get me driver's license and Dean Chueng for being a good native friend and brother. I would like to give a special thanks toward Dr. Jinping Lai. He generously let me get into his project which we completed together. He taught me numerous tricks in experiments. He showed me how to operate fluorescence spectrometer and HPLC. I feel so lucky to have such a great second mentor like Jinping in Rutgers.

I would like to thank all my friends whether they are comrades in Chemistry and Chemical Biology Department or friends outside the department. The time I spent with them are great memories which I will cherish through my life.

Last but not least, I would like to express my deepest gratitude to my family. Their support and dedication allow me to have this wonderful opportunity to be here. There is

no word I can use to express my genuine feeling toward them, but I always know that they know how much I love them.

Table of Contents

List of Figures

List of Tables and Schemes

Chapter 1

Introduction

1.1 Fluorescence and fluorescent emitters

Fluorescence is a type of photoluminescence arising from excited singlet electronic states following absorption of light[1]. The mechanism of fluorescence can be clarified with the help of Jablonski Diagram (**Figure 1.1**). When a molecule, atom or nanostructure absorbs photons or other energy, the electrons at ground state (S_0) will be excited to a higher quantum state (S_1 or S_2). Then the electrons at the higher quantum states can relax back to S_0 by emitting photons. Fluorescence is generated during this process. Also, because of the existence of vibrational energy levels, the electrons at higher quantum states can undergo non-radiative relaxation in which the energy is dissipated as heat. Due to this effect, the emitted light in fluorescence usually has a longer wavelength and lower energy than the absorbed light which is called Stokes shift[2]. But if the absorbed electromagnetic radiation is intense enough, absorption of two or more photons is possible resulting in a shorter wavelength and higher energy of emitting light. The lifetime of fluorescence can be described as a first-order reaction: $[S_1] = [S_1]_0 e^{-\Gamma t}$ where $[S_1]$ is the concentration of excited state molecules at time t, $[S_1]_0$ is the initial concentration and Γ is the decay rate[3,4]. For commonly used fluorescent compounds, typical lifetimes are no more than 100 ns[4]. In addition, a competing pathway called intersystem crossing (ISC) exists when the electron stays in higher quantum states. When ISC occurs, the electron will convert to triplet state (T_1) first, then goes back to S_0, releasing photons. This process will generate phosphorescence. Due to the longevity of T_1 state, phosphorescence usually has longer lifetime than fluorescence.

The occurrence mechanism and short lifetime of fluorescence make it can be temporal and spatial controlled. Therefore, fluorescence microscope has become indispensable tools for the studies of non-destructive tracking, dynamic molecular interaction, real-time drug monitoring, and super resolution microscopy[5-8] etc. (**Figure 1.2**). In fluorescence microscope techniques, a

fluorescent emitter is placed with the specimen. A light of specific wavelength is used to illuminating the fluorescent emitter to construct the image of the specimen. Therefore, fluorescent emitter is of great interest and importance in fluorescence microscope.

Typically, a fluorescent emitter has a dark state and a bright state. However, the ones that have two bright state with different fluorescence wavelength can also be used in fluorescence microscope[9,10]. Based on the structure of emitter, the fluorescent emitter can be divided into three broad categories: fluorescent proteins (FPs), inorganic nanomaterials and organic fluorophores.

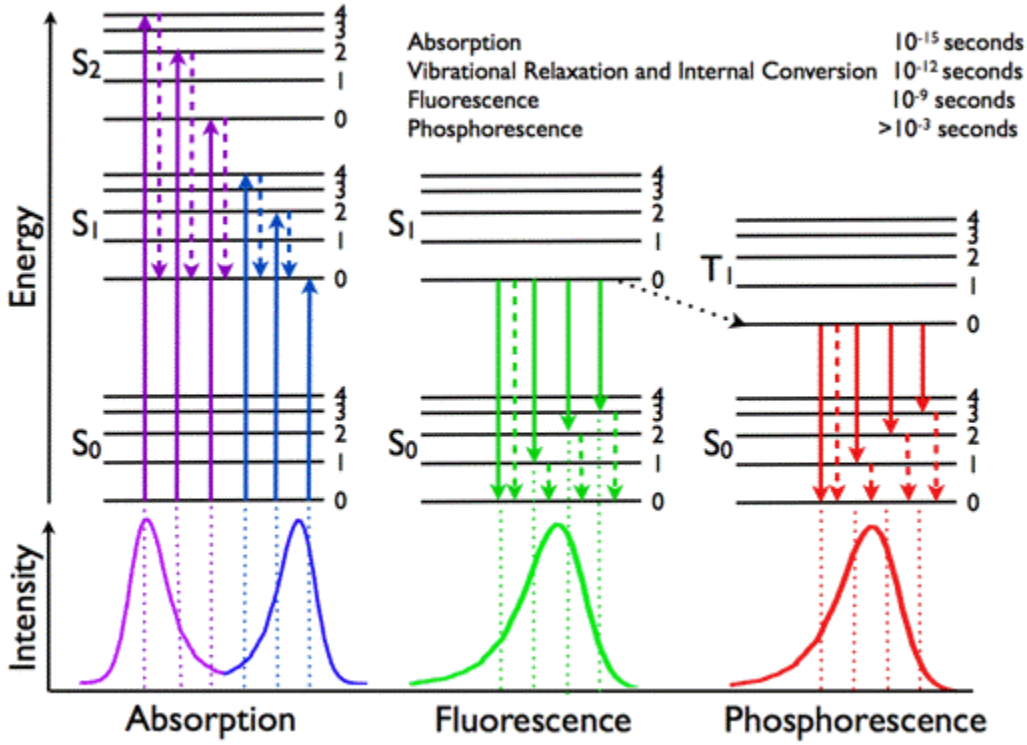

Figure 1.1 Jablonski Diagram of fluorescence and phosphorescence.

1.1.1 Fluorescent proteins

FPs are genetically encoded fusions of cellular proteins with green fluorescent proteins (GFP). GFP was first been purified from Aequorea victoria by Osamu Shimomura in 1960s[11]. It is a composed of 238 amino acid. It was then in 1990s that GFP was adopted as a marker for gene expression by several groups[12-14].Wild type GFP has a major excitation peak at 395 nm and a

minor excitation peak at 475 nm which is not preferable in studies. Besides, wild type GFP has several other drawbacks such as poor quantum yield, poor photostability and pH sensitivity[15,16]. To overcome these drawbacks, many different mutants of GFP have been engineered including but not restricted to blue fluorescent proteins (BFP)[17], yellow fluorescent proteins (YFP)[18] and cyan fluorescent proteins (CFP)[19].FPs can not only be introduced to the targets by gene expression. It can also label the targets through the use of polypeptide or through their fusion to proteins[9]. The targets of FPs are various, from single cell to subcell organelles. Even smaller molecules such as proteins and nucleic acids can be the targets too.

1.1.2 Inorganic fluorescent nanomaterials

Nanomaterials refers to a vast variety of different materials with size within 1-100 nm. Inorganic fluorescent nanomaterials includes gold nanoparticles (AuNPs), quantum dots (QDs), nanoparticles containing organic fluorophores and upconversion nanoparticles (UCNPs)[20].These materials have several advantages:

(1) Inorganic fluorescent nanomaterials have superior brightness and photostability compared to the counterparts of either FPs or organic fluorophores. This is essential for near infrared (NIR) imaging. (2)Inorganic fluorescent nanomaterials are relatively easy to synthesize. Unlike FPs and organic fluorophores which usually require a long synthetic route, inorganic fluorescent nanomaterials can be easily synthesized by well-established methods. (3)The fluorescence profile of inorganic fluorescent materials are highly tunable. By changing the size of ZnS-$AgInS_2$ QDs, Subramaniam et al. obtained a library of quantum dots of different emission wavelengths for cellular imaging[21].

AuNPs have a long-standing use as a biological probe due to the inert, non-toxic and biocompatible properties of AuNPs. The intriguing optical properties of AuNPs arise from localized surface plasmon resonance (LSPR), in which valence electrons in AuNPs oscillate coherently with incident light at specific frequency. Part of the energy absorbed by AuNPs is emitted in the form of scattered light, which is the basis of much AuNPs–based optical imaging.

Faulk and Taylor first introduced immunogold staining in 1971 for electron microscopy (TEM, SEM) of bio-samples[22]. Mirkin and his coworkers investigated the colorimetric detection of polynucleotides based on the plasmon-plasmon interactions between adjacent AuNPs[23]. With precise control of size of AuNPs, different optical resonance of AuNPs can be varied over hundreds of nm in wavelength[24].

QDs are nanosized semiconductors composed of binary alloys of IIB-VIA (e.g. CdSe) group or IIIA-VA (e.g. InP) group elements. QDs have a unique property called quantum confinement which will affect the bandgaps of QDs leading to different emission wavelengths. In contrast of organic fluorophores and FPs, QDs have a narrow emission peak. Therefore, multiple QDs with different emission wavelengths can be excited simultaneously without influence each other, realizing multicolor fluorescence imaging[25]. Better temporal control of the fluorescence of QDs was achieved by capping certain aromatic groups on the surface of the QDs[26]. Upon the illumination of UV lights, the aromatic group was cleft and the fluorescence of QDs was resumed. Another important application of QDs is NIR imaging. In traditional fluorescence microscope technology, UV or visible light is the excitation light. However, due to the inherent disadvantages with UV light, this technology has the problems of shallow penetration depth and is potentially harmful to living cells. Thus, UV light excited fluorescence microscope is not suitable for in *vivo* imaging. NIR on the other hand can penetrate deeper into tissues than UV light and is less harmful. Although there are reports of organic fluorophores and FPs capable of NIR imaging, the photostability of these emitters still present as a big problem. On the other hand, the NIR imaging using inorganic fluorescent nanomaterials has been well established. Kim et al. first demonstrate the use of CdTe@CdSe NIR QDs to map sentinel lymph nodes in mouse and pig[27]. The application of NIR QDs was reviewed in detail by many groups[28,29].However, the use of heavy metals and potential toxicity of nanocrystals may hamper the in vivo use of QDs.

UCNP is another category of inorganic fluorescent nanomaterial that has been widely used for NIR imaging[30,31]. Upconversion is a multi-photon process where lower-energy excitation

is converted to higher-energy emission which can be observed mainly in lanthanides due to the partially filled 4f inner shell of trivalent lanthanide cations (Ln^{3+}). First discovered by Auzel in the 1960s[32], UCNP quickly became a promising tool in biostudies. Generally, there are three kinds of mechanism in UC process: excited-state absorption (ESA), energy transfer upconversion (ETU) and photon avalanche (PA). All these processes involve the population of a highly excited state by sequential absorption of two or more photons[33]. Typical UCNP contains a crystalline host material and a dopant (emitter) added in low concentration. The host materials should ideally have low lattice phonon energies and good stability. The most promising hosts for UCNP are found in fluoride containing materials (e.g. $NaYF_4$) owing to their low phonon energy, high refractive index and good thermal stability. The emitters in UCNP are $Ln^{3+}$for example, Er^{3+}can absorb photons with wavelength around 1500 nm and produce four upconversion bands with wavelengths of 980, 810, 660 and 550 nm respectively. Since the emission intensity is determined by the distance between two neighboring Ln^{3+}, increasing the concentration of Ln^{3+} is a good way to improve the emission intensity. However, at higher dopant concentrations cross-relaxation become a severe problem that quenches the excitation energy[34]. To deal with this problem, a second dopant called sensitizer is co-doped to the host lattice in large concentration. Sensitizer will first absorb the energy from photons, then transfer this energy to its nearby emitters. Yb^{3+} is the most commonly used sensitizer in UCNP. It has a simple absorption band at 980 nm, corresponding to the $^2F_{5/2} \rightarrow {}^2F_{7/2}$ transition of Yb^{3+}, which is well cross-sectioned with Er^{3+}, Ho^{3+} and Tm^{3+}. Yet, with the help of sensitizer, the quantum efficiency of state of art UCNP is still well below 10% and need to be improved. Besides, broadband absorption UCNP[35,36] and multicolor UNCP[37,38] are other potential directions that are being investigated.

1.1.3 Organic fluorophores

Organic fluorophores are natural or synthetic organic compounds, which are one of the earliest fluorescent materials discovered by people as well as the first compounds used in fluorescence microscopes[1]. Generally, organic fluorophores have broad absorption band and

emission band due to the presence of vibrational energy levels. Basic requirements for an organic molecule to be fluorescent includes large conjugation system, rigid plane etc. The fluorescence profile of organic fluorophores can be adjusted by modifying the structure of the molecule. Owing to the early discover and longtime development, there is a huge library of organic fluorophores and many of them have been commercialized (e.g. Alex Fluor). The details of organic fluorophores will be discussed in section 1.2.

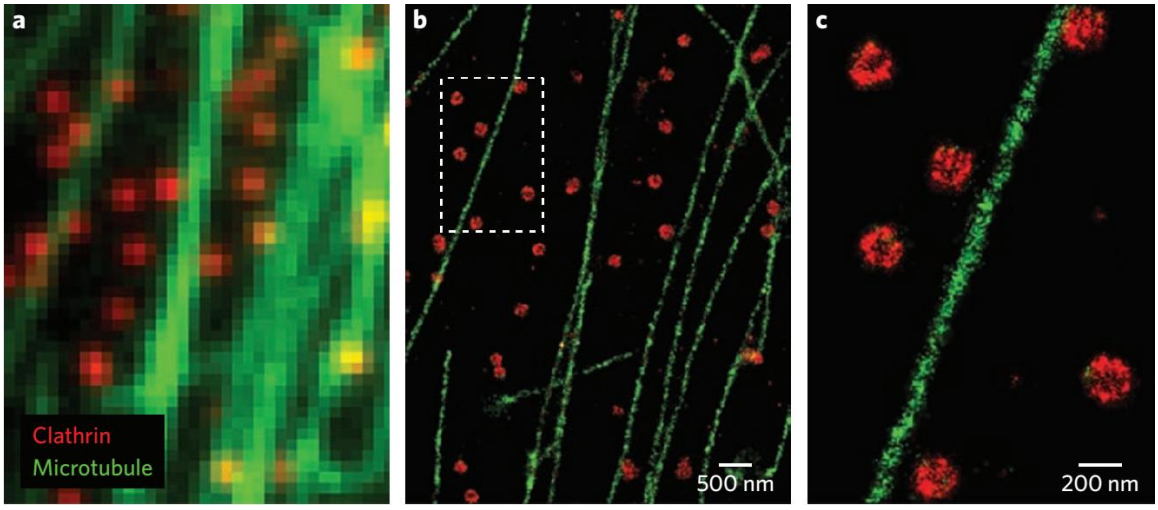

Figure 1.2 a, Conventional fluorescence image. b, Super resolution microscopic image of the same area. c, Magnified view of the boxed region in b.

1.2 Photoactivatable synthetic organic fluorophores

Organic fluorophores can be put into two categories: reversible fluorophores and irreversible fluorophores based on whether the fluorophores can switch between the dark state and bright state. Reversible fluorophores or photoswitchable fluorophores undergoes reversible photoswitching under different wavelengths. Photoswitchable fluorophores are the pivotal components in super resolution microscopy. The mechanism of photoswitch involves the break and reform of a bond that will render rigidity or the conjugation of the system. For example, in the case of cyanine dye Cy5, red light will trigger the photochemistry of Cy5 adding a thiol group to one of the double bonds, breaking the conjugation of Cy5 molecule, turning it to dark state. Upon illumination of the light with another wavelength, the reverse reaction will happen, losing the thiol group and resuming the fluorescence[39].

Irreversible fluorescent emitters are masked by a photolabile protecting group (PPG) to stay at a stable dark state. This stable dark state can be subsequently photoactivated to a fluorescent state for high photon emission through the cleaving of PPG. Therefore, this kind of fluorescent emitters is also called photoactivatable fluorophores.

1.2.1 Photolabile protecting groups

In photoactivatable fluorophores, the PPG plays a role as cage that can quench the fluorescence of the fluorophore. The criteria for a common good PPG includes: (1) it should have strong absorption at wavelength well above 300 nm to avoid the absorption by biological entities. (2) The cleavage photoreaction should be clean and should occur with a high uncaging yield (Φ_{unc} which is equal to the amount of released substrate divided by the amount of photons at the irradiation wavelength that were absorbed by the caged compound). (3) The PPGs must be stable in the media prior to the photolysis. (4) The photochemical byproducts accompanying the released bioactive reagent should be transparent at the irradiation wavelength. (5) The PPGs must be biocompatible. Depending on the specific situations, the PPGs may need to be able to pass through biological barriers such as membranes and show affinity to the target[40]. After years of

development, dozens of PPGs emerged including nitroaryl groups, arylcarbonymethyl groups, phenylazides and so on. These days, *o*-nitrobenzyl and nitrophenethyl based PPGs are the most commonly used PPGs. They can be used to release esters, amides, carboxylic acids, alcohols, thiols etc. upon illuminating. The primary photoreaction of an *o*-nitrobenzyl-based PPG was carefully studied[41]. It was stated that the mechanism starts with the transfer of a proton from the benzyl substituent to nitro group, forming an aci-nitro tautomer. Then this tautomer undergoes intramolecular nucleophilic addition to form a bicyclic intermediate product who subsequently open the ring and release the protected fluorophore. The best part of *o*-nitrobenzyl PPGs is the properties of these compounds can be further tuned by modifications. For example, one can add substitution groups at the benzylic position or on the aromatic ring to increase the quantum yield of the PPGs, the rate of release and absorbance at longer wavelengths. However, during the uncaging process *o*-nitrobenzyl-based PPGs generate *o*-nitrosobenzoyl byproducts which is the major drawback of *o*-nitrobenzyl-based PPGs because *o*-nitrosobenzoyl is not only cytotoxic, but also strongly absorbing.

Arylcarbonylmethyl PPGs are aromatic ketones in which the carbonyl group is usually the center of the photochemical reactivity. They are typical of the PPG framework for release of carboxylic acids. The transfer from photo-excited S_1 state to T_1 state plays a crucial role in photoactivation process of these PPGs. This may be rationalized by the energetically close lying states (n, $\pi*$ and π, $\pi*$) in aromatic ketones, leading to a very fast and efficient ISC[42,43]. In many cases of arylcarbonylmethyl PPGs, photogenerated enols are believed to be the intermediate before releasing of the leaving groups. After photoactivation, the byproducts of arylcarbonylmethyl PPGs are usually aromatic ketones which are highly phosphorescent and only weakly fluorescent. That's another advantage these PPGs have.

The photolysis reaction of aryl azides, eliminating a nitrogen molecule and forming a highly reactive nitrene has been well studied decades ago[44]. Although azide-based fluorophores have been reported before[45],it was until recently that this reaction was applied to construct

photoactivatable fluorophores for labeling and super resolution imaging[46-49]. The photolysis of azides is a very clean reaction because the sole byproduct is nitrogen gas which can quickly release to the environment leaving no effect to the system we want to study. The other product nitrene can subsequently insert into bonds of surrounding molecules or form azepine via intramolecular ring-expansion. However, an electron push-pull effect is required after the generation of fluorophore to obtain strong fluorescence which makes the application of aryl azide PPGs to very limited examples.

Besides removable fluorescence quenchers, photoinduced cycloaddition can also be used as the strategy to construct a photoactivatable fluorophore which can be treated as a broader sense of PPG. Yu and his coworkers designed a microtubule-binding photoactivatable fluorescent probe[50]. In this design, photoinduced click reaction between tetrazole and alkene is the key for fluorescence generation.

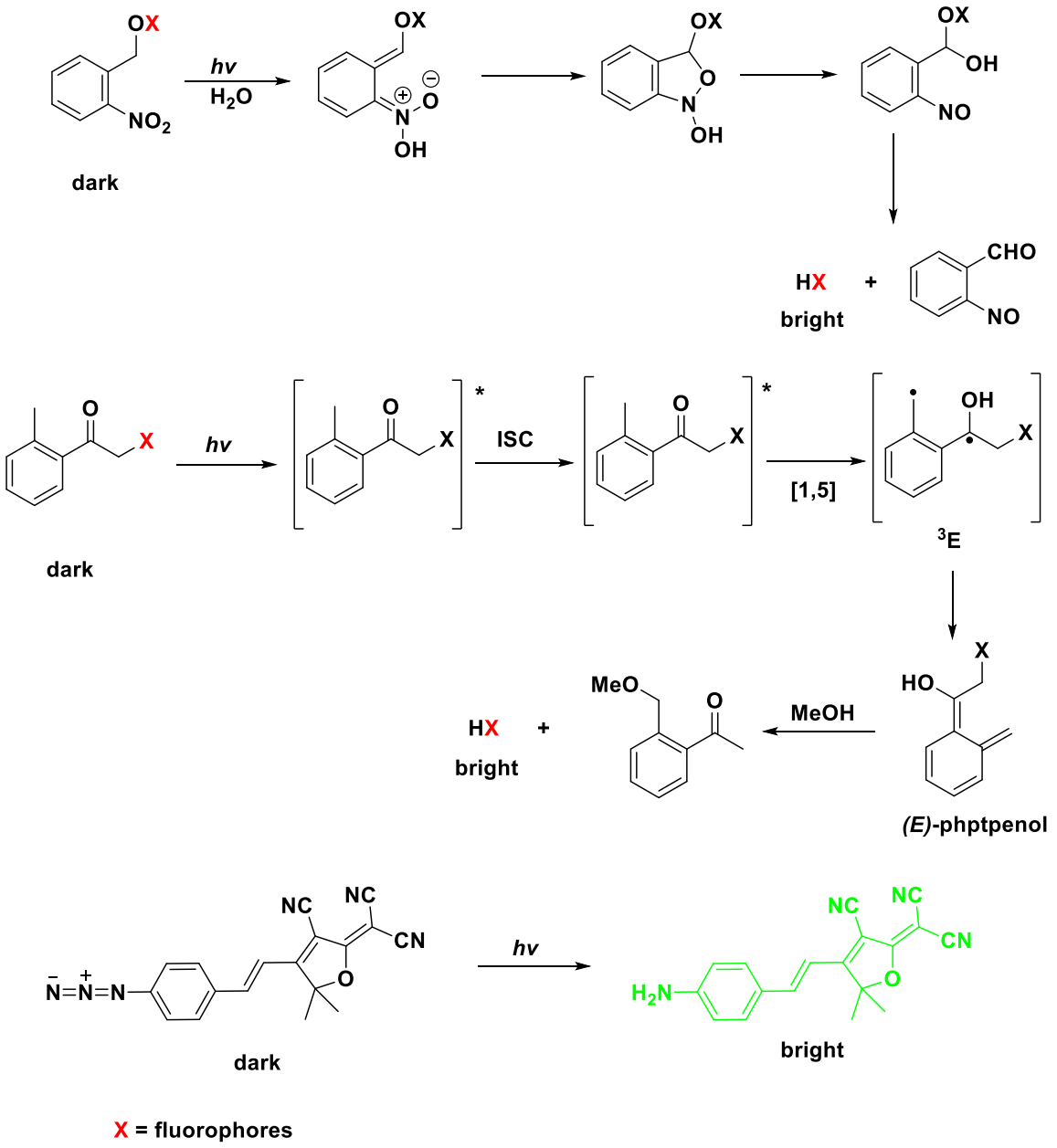

Scheme 1.1 Uncaging mechanisms for o-nitrobenzyl, arylcarbonylmethyl and aryl azides PPGs.

1.2.2 Organic dyes

The other part in photoactivatable organic fluorophores is the fluorescent core which usually is an organic dye. Organic dyes are often compared with FPs because these two fluorescent emitters can be used in photoactivatable and photoswitchable fluorophores. Unlike the FPs which were discovered and developed only for decades, the first organic fluorophore was

described in 1565. Compared to FPs, the synthesis of organic dyes is relatively simple. The well-developed organic synthesis also makes it relatively easy to add all kinds of functional moieties to the original dyes to modify their fluorescence profiles. The small molecular size of organic dye is expected to cause less perturbation on protein functions or activities. What's more, the emergence new protein labeling strategies such as HaloTag[51] and SNAP-Tag[52] makes it possible to label proteins with organic dyes with excellent specificity and fast kinetics. Even in certain cases, for example, cell-cell coupling through gap junction channel only allow organic dyes that are small enough to pass. Those reasons make the relationships between organic dyes and FPs more like complementary. Over the long history between human and organic dyes, hundreds of organic dyes were prepared. Here, I will give a brief introduction to some of the most used organic dyes today in laboratories.

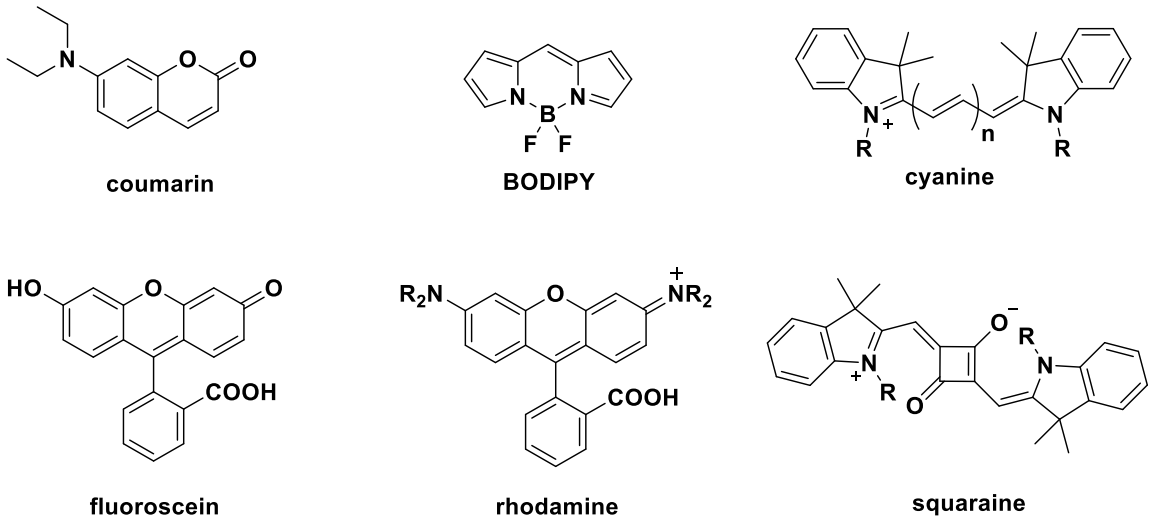

Scheme 1.2 Structure of some commonly used fluorescence cores.

Coumarin is a class of compound that is originally found in many plants. One can also obtain coumarins in laboratories using several name reactions such as Pechmann condesation reaction between phenol and carboxylic acid or ester[53]. Compounds in this class all contain a 1-benzopyran-2-one core. Owing to their small molecular weight, high quantum yield and water solubility, coumarins are widely used for biolabelings. But, the emission band of coumarin and its

derivatives are usually below 500 nm (blue light) and the fluorescence intensity may not as good as other dyes, which limits their further applications. Zheng and his collaborators designed a photoactivatable using coumarin and fluorescein linked through a 1,4-diaminocyclohexane[54]. In this dye, excited coumarin can transfer its energy to the fluorescein through Förster resonance energy transfer (FRET), thus changing the emission band from coumarin to that of fluorescein (520 nm). This method provides a good way to prepare longer emission wavelength coumarins.

Fluorescein is a polycyclic dye belongs to xanthene. Fluorescein derivatives are the most common fluorophores for biological researches. They may be synthesized from phthalic anhydride and resorcinol via Friedel-Crafts reaction[55]. Fluorescein possesses the advantages of high molar absorptivity, excellent fluorescence quantum yield and good solubility in water. By adding an isothiocyanate group, the popular fluorescein derivative FITC for protein conjugation is obtained[56]. Another important fluorescein derivative is the biarenical fluorescein. Fluorophores in this family are developed for the in vivo specific labeling of target peptides or proteins. This approach, developed by Griffin et al. exploits the facile and reversible covalent bond formation between organoarsenicals and pairs of thiols[57]. Fluorescein dyes may display some disadvantages including high rate of photobleaching, pH-sensitive fluorescence, broad fluorescence emission spectrum and self-quench on conjugation to biopolymers.

Rhodamine is another member of xanthene dyes. One can use similar synthetic strategy to that of fluorescein to prepare rhodamines in labs. Rhodamine dyes are among the oldest synthetic dyes used for dyeing of fabrics. These dyes often have high molar absorptivity in visible region and strong fluorescence beyond 500 nm. The fluorescence profile of rhodamines are strongly influenced by substituents in the xanthene core. Popular rhodamine dyes include Rhodamine B, Rhodamine 6G and Rhodamine 123. Rhodamine dyes are generally soluble in water which enables them to be used in studies of localizing proteins, enzymatic activities and others. Since rhodamine dyes are generally toxic, it is extremely important to establish the extent to which the dye changes the behavior of target biomolecules.

Cyanine dyes are synthetic polymethine (conjugated carbon double bonds) dyes. The basic structure includes two aromatic or heterocyclic rings linked by a polymethine chain. Longer polymethine chain will lead to longer excitation wavelength. Therefore, these compounds are by far the main source of organic long-wavelength fluorophores and provide excitation bands in the range of 600-900 nm. The synthesis of cyanine dyes is very straightforward and generally accomplished by the stepwise reaction of nucleophilic heterocycles with a polymethine chain precursor[58]. Cyanine dyes are of particular interest to fluorescence microscopy due to their high molar extinction coefficients, broad wavelength tenability and NIR absorption. Most cyanine dyes suffer from the problem of poor water solubility. But this can be mitigated by the introduction of alkyl sulfonate groups. Cyanine dyes are good photoswitchable fluorophores which undergo reversible thiolation reaction in different wavelengths[39]. Because of this property, the most important application of cyanine dyes is probably on Stochastic Optical Reconstruction Microscopy (STORM)[59].It is worth to mention that some cyanine undergo an intrinsic photochemical process where the dye is decomposed through a regioselective photooxidative C-C cleavage reaction. This reaction, historically a liability however, is exploited by Gorka et al. to provide the scaffold of a cyanine based photoactivatable fluorophore[60].

Squaraine is another subclass of polymehine dyes. Like cyanine dyes, squaraines are used as fluorescence probes in NIR. They have extremely intense and sharp absorption and emission bands. Squaraines can be derived from squaric acid, which undergoes an electrophilic aromatic substitution reaction with aniline or other electron rich derivatives. Structural modifications in these compounds can be achieved by introduction of substituents into the aromatic ring or on the N atom of the terminal heterocyclic moiety. It is also possible to modify the squaraine ring, but this is more difficult. Such changes can be used to produce a red shift of the absorption and fluorescence bands.

Boron-dipyrromethene (BODIPY) is a class of long-wavelength dye. The core of BODIPY is a dipyrromethene complexed with a disubstituted boron atom. Generally, BODIPY

dyes have high molar extinction coefficients, high quantum yield, good photostability and narrow emission band widths. Another worth-mention advantage of BODIPY dyes is their insensitivity to solvent or pH. The fluorescence profile of BODIPY can be tuned by modifications of the pyrrole core.

1.3 Conclusion

Fluorescence microscope has become crucial tools in scientific studies especially in biological studies ever since its emergence. In the past decades, many new fluorescence microscope techniques were designed to meet the increasing requirements of biological analysis tools. As an important component in all fluorescence microscope technologies, fluorescent emitters determine the precision and availability of fluorescence microscopes. Although the discovery of FPs and application of nanomaterials in fluorescence microscope greatly extend and improve library of fluorescent emitters, organic fluorophores still plays an irreplaceable and central role in many fluorescence microscope techniques. Photoactivatable fluorophores provide scientists spatial and temporal control over the fluorescence. Owing to this ability, designing photoactivatable fluorophores which have superior fluorescence profile and uncaging efficiency has become one of the most dynamic researching areas in recent years. However, many organic synthetic dyes we used today may involve complicated organic synthesis and unintended loss of bioactivity due to the structural modifications. In addition, commonly used *o*-nitrobenzyl PPGs suffer from several problems including reduced photo-activation efficiency due to the filtering effect of the latent fluorophores and cytotoxicity of the photolysis by-products. Hence, development of new uncaging strategy with high activation efficiency as well as design of new fluorophores flexible in their synthesis and bioconjugation present as a promising challenge.

Chapter 2

N-Hydroxyoxindole-Based Photoactivatable Fluorophores for bioimaging

2.1 Introduction

Photoactivatable fluorophores which exist in stable dark states, but can be subsequently photoactivated to a fluorescent state for high photon emission,[61] are crucial tools for advanced microscopy imaging, such as super-resolution imaging[62] as well as for investigating dynamic biomolecular processes in living cells. Due to their exquisite spatiotemporal control over fluorescence by using light.[63] To date, several strategies have been reported for the design of photoactivatable fluorophore, including the photo uncaging of "caged" conventional fluorescent dyes (e.g., fluorescein, rhodamine) and FRET-based dyes,[64-68]photo-release of fluorophores from fluorescence quenchers;[69,70] photo-switching of the spiropyran-merocyanine based nanoparticles;[71,72] and the intramolecular photoclick reaction of tetrazole-alkene.[73] However, the above-mentioned strategies suffer from several limitations, including reduced photo-activation efficiency due to the filtering effect of the latent fluorophores and cytotoxicity of the photolysis by-products seen in commonly used *o*-nitrobenzyl-based caged dyes[74-77]. Additionally, design and development of such photoactivated fluorophores may involve complicated organic synthesis and unintended loss of bioactivity due to the structural modifications. Hence, it is important to develop a more biocompatible photoactivatable fluorophore with high activation efficiency as well as greater flexibility in their synthesis and bioconjugation for realizing their widespread potential in advanced imaging techniques.

In this communication, we report the development of a new class of photoactivatable fluorophore based on a substituted *o*-nitrophenyl ethanol (ONPE) structure, capable of rapid and ultra-efficient photoactivation (up to 800-fold fluorescence turn-on ratio) with negligible inner-filter effect and minimal cytotoxic side products. In contrast to the conventional caged dyes, our

self-caged fluorophore is substantially small in size (single benzene moiety *vs* 3-4 benzene moiety-based conventional dyes, such as fluorescein and rhodamine) and therefore involves facile synthesis and minimal steric perturbation in biological systems, which is of particular importance when probing dynamic molecular processes.[78] Furthermore, we demonstrate a structure-activity relationship between the different substituted ONPEs and their corresponding fluorescent properties, which can serve as a guideline for the design and development of new photoactivatable fluorophores with desired optical properties. Finally, we demonstrate the application of a photoactivatable dye with excitation-emission in green-red region for spatially-controlled imaging of human neural stem cells (hNSCs) and cervical cancer (HeLa) cells.

2.2 Results and Discussion

2.2.1 The fluorescence profile of ONPE photoactivatable fluorophores

As shown in **Figure 2.1A**, the photoactivation reaction in our system is based on an intramolecular photocyclization of ONPE. Photo irradiation (λ = 254 nm) of ONPE leads to the selective oxidation of the ethanol group to acetic acid by the excited nitro group, followed by the cyclization of the intermediate to form *N*-hydroxyoxindole and water as the side product. We found that 5-methoxycabonyl ONPE which is non-fluorescent in solution (3:1 v/v, methanol/PBS, pH 7.4, 10 mM) would generate strong fluorescence in the same solution after brief exposure to UV light (254 nm, 3 $mW \cdot cm^{-2}$, 1 min). By monitoring the absorption spectrum of this reaction as a function of time, it was revealed that the photolysis proceeds with a decrease in the absorption peak of 5-methoxycabonyl ONPE at 254 nm and a concomitant formation of a new strong absorption peak centered at 324 nm (. This is accompanied by a remarkable up-to-800-fold fluorescence enhancement with the maximum emission peak at 520 nm. The photolysis process was further monitored by HPLC-MS, which showed a major product with a molecular weight of 5-methoxycarbonyl *N*-hydroxyoxindole (207.2 g/mol). These results indicate the photoreaction of ONPE is clean and rapid.

To understand the structure-activity relationship of this photoinduced fluorescence, we synthesized a series of ONPEs with different substituted groups and studied the fluorescence profiles of their respective photoreactions. As summarized in Table 1, only the compounds with strong electron withdrawing groups (EWG) such as carbonyl and cyano groups (entry **1**-**4**) showed significant fluorescence enhancement after photo-irradiation. In particular, **1** which possesses a methyl acetate group, demonstrated a large difference in absorption peaks before and after photo irradiation (254 nm *vs* 334 nm), and a large Stokes shift (186 nm) as well as an 800-fold fluorescence enhancement. The hydrolysis of the substituted methyl acetate in **1** to acid (entry **6**) led to a photolysis product with a weak fluorescence. It should be noted that only a negligible fluorescence enhancement was observed in case of non-substituted ONPE (entry **7**) or

compounds with strong electron donating groups(EDG) such as methoxyl group (entry **8, 9** and **10**). Furthermore, photolysis of the derivatives such as the esterification product of ONPE led to generation of non-fluorescent *o*-nitrostyrene. These results reveal a strong structural significance of the 4' or 5'-substituted strong EW groups and 1'-unmodified ethyl hydroxyl group for the high sensitive photoactivation of ONPE with strong fluorescent *N*-hydroxyoxindole product.

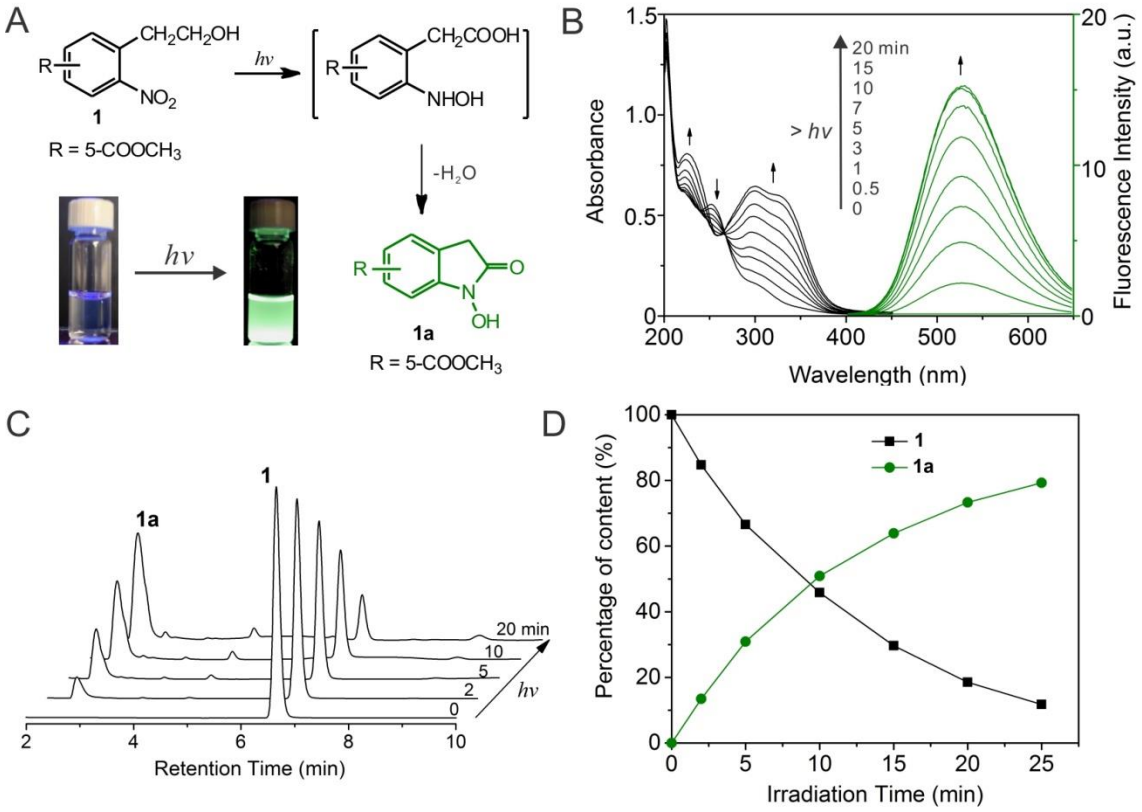

Figure 2.1 (A) Photocyclization of ONPE to N-hydroxyoxindole. Inset shows the photographs of a solution of **1** under UV lamp before and after UV irradiation. (B) Absorption and fluorescence spectra depicting the photolysis of **1** in MeOH/PBS (3:1, v/v) under UV light irradiation (254 nm). (C) HPLC analysis of the photolytic reaction reveals progressive photolysis of 1 upon irradiation and formation of a major photolytic product (1a). The signal was recorded with a UV-absorption detector at the wavelength of 299 nm, which is the isosbestic point of the absorption spectrum shown in (B). (D) Content analysis of the **1** and **1a** during the photolysis shows 50% symmetry indicating a clean photolysis reaction without any by-products. Analysis was done using integrated area of 1 and **1a** on the HPLC chromatogram.

We further evaluated the fluorescence properties of **1a** in detail. As shown in **Figure 2.2 A**, oxinidole **1a** has maximum absorption at 324 nm, and a broad fluorescence emission peak centered at 520 nm, with a fluorescence quantum yield of 36% in MeOH/PBS solution (3:1 v/v,

pH7.4), and an emission lifetime of 2.51 ns. The fluorescence emission was dependent on the polarity of the solvent used, with maximum emission peak shift from 516 nm to 535 nm observed when the solvent was changed from PBS (pH7.4, 10 mM) to methanol. In addition, the photophysical properties of **1a** were found to be pH-dependent. At pH lower than 4, **1a** had an absorption peak at 281 nm. However, an increase in pH (> 4) resulted in a decrease of the absorption at 281 nm, while generating a new absorption peak at 324 nm with an isosbestic point at 299 nm (**Figure 2.2B**). This pH-induced change in the absorption spectrum indicated the deprotonation of the *N*-hydroxyl moiety in **1a** as shown in **Figure 2.2D** and revealed a pK_a of 6.5. The absorption maxima peaks at 281 nm and 324 nm can be assigned to the protonated and deprotonated form of **1a**, respectively. On the other hand, fluorescence spectrum of **1a** demonstrated an emission peak at 520 nm over the entire range of pH from 3 to 10. While the emission wavelength of **1a** is pH-independent, the emission intensity is highly dependent on the solution pH as well as excitation wavelengths. As shown in **Figure 2.2C**, fluorescence quenching and enhancement following increase in the solution pH were observed using excitation wavelength of 291 nm and 324 nm, respectively. However, the emission intensity remained constant under all pH conditions when using the isosbestic point as excitation wavelength (299 nm). These results strongly suggest a photoinduced proton transfer within the excited **1a** (**1a***), where **1a*** undergoes rapid deprotonation to its fluorescent alkaline form (**Figure 2.2D**). A similar photochemical reaction has been demonstrated in the trisodium salt of 8-hydroxypyrene-1,3,6-trisulfonic acid (HOPSA),[79] a well-known excitation-ratiometric pH sensor, thus indicating the great potential of our **1a** as a new photoactivatable excitation-ratiometric pH sensor.

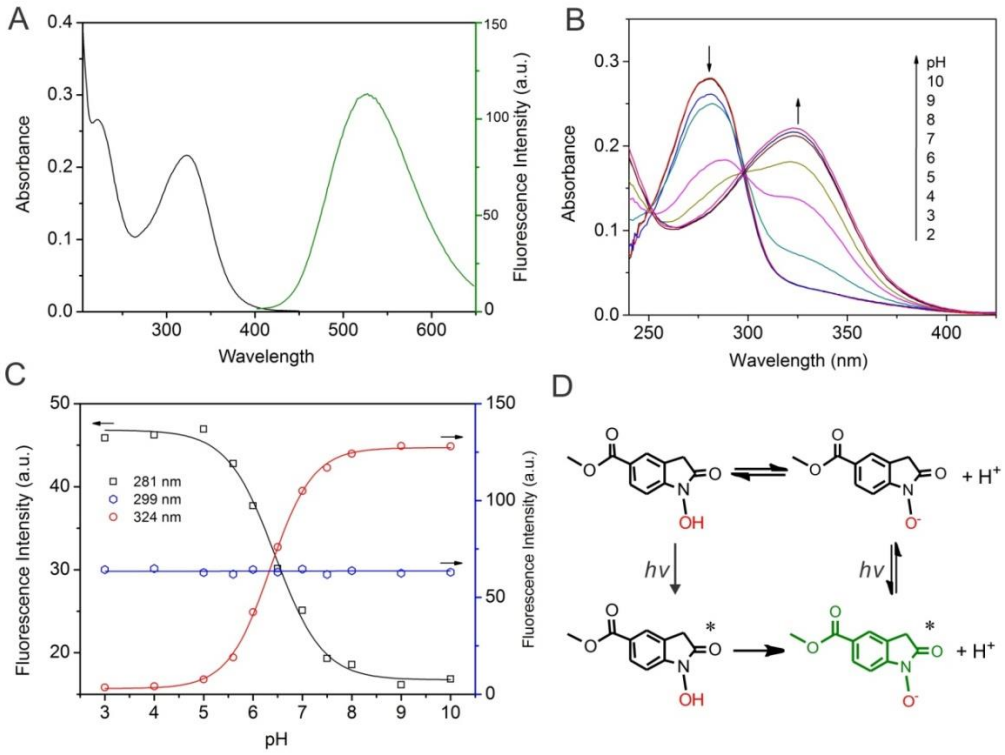

Figure 2.2 (A) Absorption and fluorescence emission spectra of **1a** in MeOH/PBS (3: 1, v/v) solution. (B) pH-dependent UV-Vis absorption spectrum of **1a**. (C) pH-dependent fluorescence emission intensity of **1a** with different excitation wavelengths. (D) Schematic illustration of the photo-induced deprotonation of the N-hydroxyl group of **1a** at excited state

2.2.2 Investigations of fluorescence generation mechanism

Based on the fluorescence profile we obtained for ONPE-based photoactivatable fluorophores, it's reasonable to further propose a photoinduced excited keto-enol tautomerization of **1a** where the enol form acts as the fluorescent molecule (**Figure 2.3**). As compared to its keto form, the enol form of **1a** has an extended conjugation and an electron pull (carbonyl)-push (hydroxyl) structure in **1a**, displaying typical intramolecular charge transfer (ICT) fluorescence and resulting in a fluorescence profile with large Stokes shift and polarity-sensitive emission.[80] Such keto-enol tautomerization for **1a** is proposed to be photoinduced and can only be observed at the excited state of **1a** and not at ground state as seen in ground-state 1H-NMR spectrum. Our hypothesis was supported by the DFT simulations, which revealed that the keto and the enol form is the thermostable molecular configuration for the ground and excited state of **1a**, respectively.

Table 2.1 Optical properties of *o*-nitrophenylenthanols with various substituted groups and their corresponding oxindoles. [a]

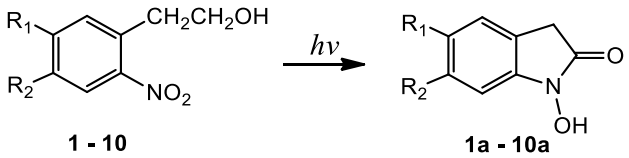

1 - 10 **1a - 10a**

Compound	R_1	R_2	λ_{max}[b] (nm)	λ_{em}[d](nm)	φ_F[e]	F/F_0[f]
1	$COOCH_3$	H	254	ND	ND	-
1a	$COOCH_3$	H	334	520	0.36	800
2	H	$COOCH_3$	230	ND	ND	-
2a	H	$COOCH_3$	290	401	0.15	200
3	$COOCH_3$	OCH_3	334	ND	ND	-
3a	$COOCH_3$	OCH_3	321	502	0.17	230
4	CN	H	254	402	0.001	-
4a	CN	H	290	514	0.047	32
5	CHO	H	258	460	0.001	-
5a	CHO	H	317	585	0.13	161
6	COOH	H	262	450	0.001	-
6a	COOH	H	282	485	0.027	21
7	H	H	260	ND	ND	-
7a	H	H	325	450	0.001	3
8	CH_2OH	H	273	ND	ND	-
8a	CH_2OH	H	321	420	0.001	3
9	OCH_3	H	312	ND	ND	-
9a	OCH_3	H	325	458	0.001	5
10	H	OCH_3	345	ND	ND	-
10a	H	OCH_3	275	457	0.002	6

[a]All the spectra were recorded in MeOH/PBS (3:1, v/v) solution with a concentration of 10 μM. [b]Absorption maxima in the 225-450 nm region. [c] Fluorescence emission in the 400-650 nm region. [e] Fluorescence quantum yields were measured using fluorescein (**1a**, **3a**, **4a** and **5a**) and DAPI (**2a** and **6a**-**10a**) as standard.[f] Obtained by comparing the integrated area of emission. ND = not detected.

To further verify this hypothesis, we synthesized methyl 3-(*tert*-butyl)-4-nitrobenzoate as a control compound (**C1**), which can be photolysed to produce a *N*-hydroxyoxindole without α-proton (**C1a**).[81] Such a molecule would therefore not undergo the keto-enol tautomerization, thus resulting in a smaller π-conjugation when compare to **1a**. As expected, a fluorescence enhancement (106-fold) in the UV region (350 nm) with a smaller Stokes shift (62 nm) was

observed for the photolysis of **C1**, indicating an emission from the local excited state of **C1a,** in contrast to the ICT fluorescence of **1a**. These results strongly support the hypothesis on the photoinduced keto-enol tautomerization of **1a** and offer a deeper understanding in the fluorescence properties of oxindole. Taken together with the importance of EWG on 5-position of benzene and the hydroxyl on ethyl alcohol, a correlation between the molecular structure and the photophysical properties could potentially serve as a guideline for the design of new ONPE based photoactivatable dyes with desired photophysical properties.

2.2.3 Photoactivatable fluorophore TCF-ONPE

As a proof of concept, we showed the development of a new ONPE-based photoactivatable fluorescence dye with excitation-emission in green-red region, which is promising for the application of spatially-controlled cell-selective imaging. As shown in **Figure 2.4A**, ONPE was substituted with a strong EW group, 2-dicyanomethylene-3-cyano-4, 5, 5-trimethyl-2, 5-dihydrofuran (TCF)[82] *via* a conjugated double bond (**11**). Therefore, the resulting photolysis product (**11a**) would not only retain the intramolecular electron pull-push property, but also has an extended conjugated system, thus endowing the dye with a longer wavelength of photolysis and excitation-emission. As expected, **11** showed broad absorption in UV to visible region, with an absorption maximum at 396 nm (**Figure 2.4B**). Upon irradiating a methanol/PBS (3:1 v/v) solution of **11** with 365 nm light, a decrease in the absorption of **11** at 365 nm and an increase in absorption at wavelength longer than 450 nm was observed, indicating the photolysis of **11**. Simultaneously, a 30-fold enhancement in fluorescence emission at 620 nm was observed with a 20 min of exposure. The

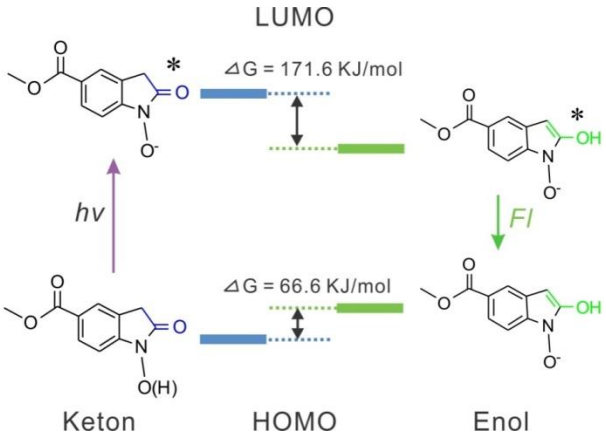

Figure 2.3 Calculated energy level diagram of 5-methoxycarbonyl-N-hydroxyoxindole

photolysis of **11** was further followed by the HPLC-MS analysis (**Figure 2.4C**), demonstrating that the photoreaction is clean and produced **11a** as the major photolysis compound, which had an excitation at wavelength longer than 500 nm and emission at 620 nm, with a fluorescence quantum yield of 2.6%. Furthermore, in contrast to the widely used photolabile *o*-nitrobenzyl compounds which show significant photolysis-induced cytotoxicity due to the formation of highly reactive *o*-nitrosobenzyl products,[74] it was expected that the ONPEs would be biocompatible due to the formation of water molecules as the only side product during the photolysis. To verify this, we evaluated the cytotoxicity of OPNE **11** and its correspondent oxindole **11a** in human neural stem cells (hNSCs) and cervical cancer (HeLa) cells using cell proliferation assays. As shown in **Figure 2.4D**, negligible effect on cell viability (>80%) was observed for both **11** and **11a** over a wide range of concentrations (0-50 μM) Overall, these results indicated that the new developed photoactivatable fluorophore **11** has great potential for cell-selective imaging related bio-applications.

We further examined the intracellular photoactivatable properties of 11. As shown in **Figure 2.5A**, HeLa cells incubated with 11 (5 μM) showed negligible fluorescence before UV activation (t=0). However, a dramatic time-dependent fluorescence enhancement was observed once the cells were irradiated with UV (**Figure 2.5A-G**). A 3 min UV exposure led to a 30-fold fluorescence enhancement of the cell while without any significant photobleaching **(Figure 2.5E)**, thus highlighting the robust photostability of **11a**.

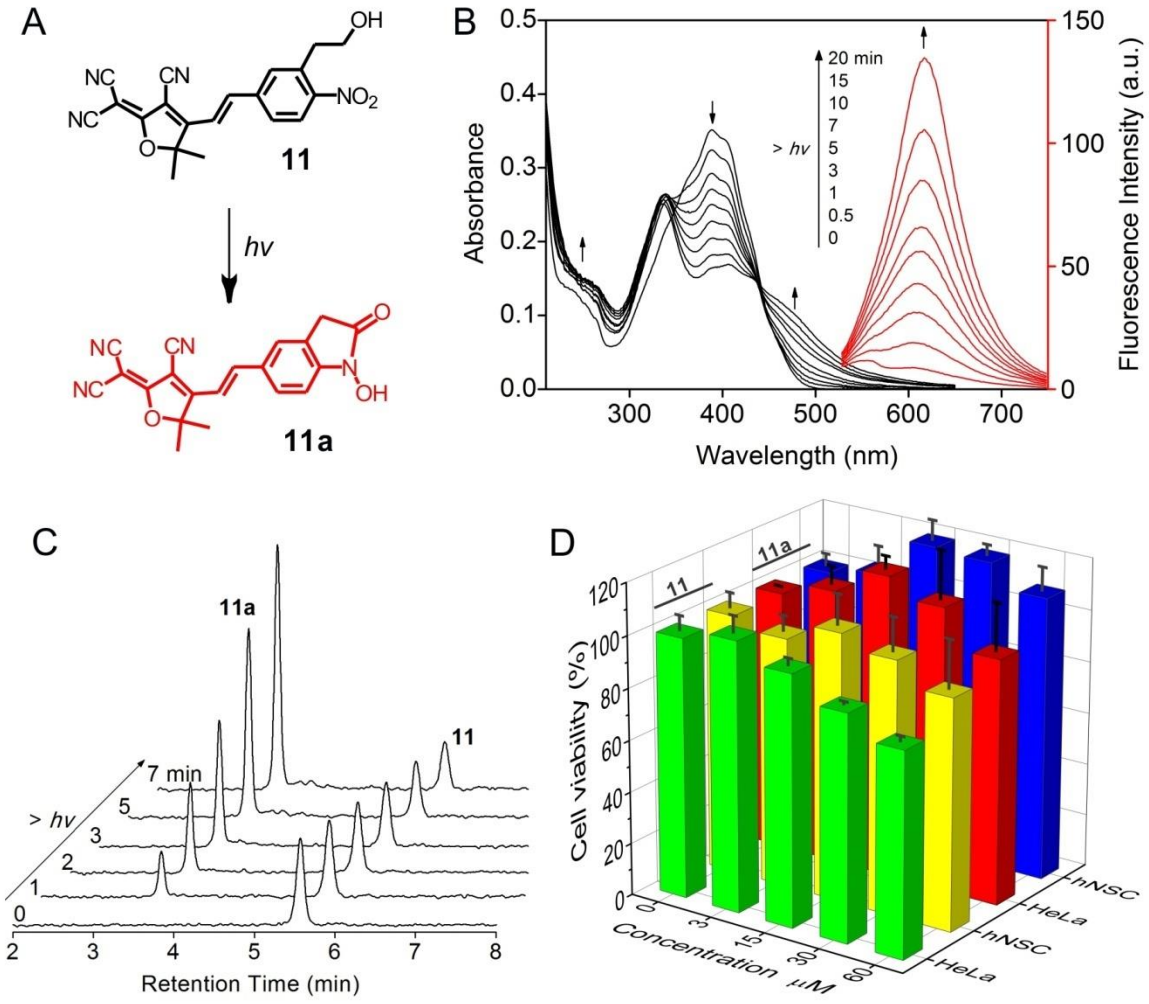

Figure 2.4 (A) Molecular structure of the photoactivatable dye **11** and its corresponding photolysis product **11a**. (B) UV-Vis absorption and fluorescence emission spectra analysis of the photolysis of **11** in MeOH/PBS (3:1, v/v) under UV light irradiation (photolysis, 365 nm, 3 $mW \cdot cm^{-2}$; excitation, 480 nm). (C) HPLC monitoring revealed that the photolysis is clean and produces **11a** as the major product. (D) Analysis of viability and proliferation of HeLa cells and hNSCs in the presence of increasing concentrations of **11** and **11a**.

Finally we went on to establish whether we could spatio-temporally control cell imaging. As shown in **Figure 2.6**, only the cells unprotected by photomask showed remarkable fluorescence after UV exposure. We further demonstrated the enhanced spatially-controlled single cell-selective imaging utilizing a confocal microscope. The broad absorption band of **11** enabled the photo activation to proceed at 405 nm irradiation. As demonstrated in **Figure 2.4D**, only the selected hNSC irradiated with blue light (405 nm, 15 s) showed bright red fluorescence,

indicating successful rapid fluorescence enhancement of **11a**. In contrast, the region beyond the selected cell demonstrated weak fluorescence enhancement (16% intensity as compared to the activated region).

2.2.4 Conclusion

In conclusion, we have developed a new class of photoactivatable fluorescent probes based on substituted *o*-nitrophenyl ethanol (ONPE) structures. These self-caged fluorophores are small in molecular size, show ultra-high (up to 800-fold) photo-induced fluorescence enhancement with good biocompatibility and hence can be readily adopted for applications such as monitoring dynamic molecular processes in living cells. Furthermore, we have revealed a structure-activity relationship between the substituted ONPE probes and their corresponding emission profiles, which can serve as a guideline for designing fluorescent probes with desired photophysical properties. As a proof of concept, an ONPE derivative with Vis excitation (>500 nm) and NIR-emission (620 nm) has been developed and its application in the spatially-controlled selective labeling of single cancer and stem cells has been demonstrated. Thus, the developed ONPE based caged fluorophores can eventually evolve into valuable probes for the convenient super-resolution imaging of biological samples and thereby permitspatiotemporally controlled mapping of biomolecular processes.

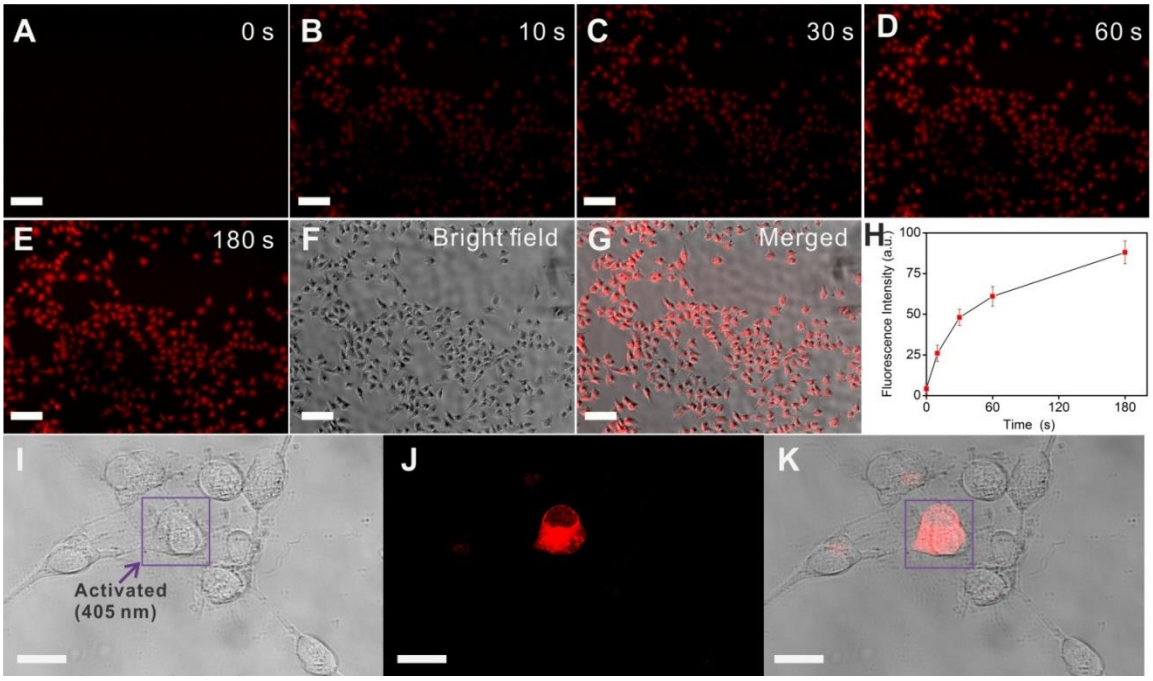

Figure 2.5 (A-H) Time-dependent photoactivation of **11** in HeLa cells. The photoactivation was performed on a Nikon Ti microscope using the DAPI excitation (Nikonen slight C-HGFI lamp, 130 W) with a 20X objective lens. The fluorescent images were collected using Texas Red channel (excitation 550-580 nm, emission 600-650 nm). Dye concentration is 5 μM, scale bar is 100 μm. (I-K) Spatially-controlled photoactivation of **11** in hNSCs. (I) DIC, (J) fluorescence, and (K) merged images of a single hNSC with photoactivated fluorescence. The selected cell was first irradiated by a 405 nm excitation from the confocal microscope (5.95 mW, 15 s) and the fluorescence imaging was recorded with an excitation at 515 nm. Scale bar is 20 μm.

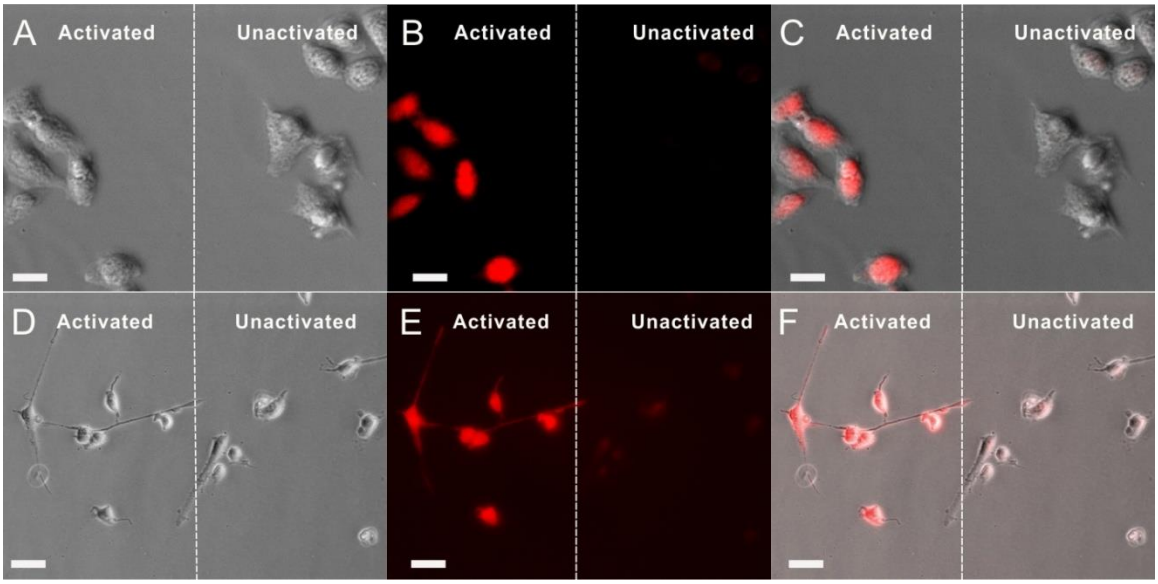

Figure 2.6 Photomask-assisted spatially-controlled cell-selective imaging of HeLa cells (A-C) and hNSCs (D-F). Bright field images (A and D), fluorescent images (B and E) and their emerged images (C and F). UV-activation was carried out by using the UV excitation channel of the microscope (exposure time was 30 s). Fluorescent images were collected using Texas Red channel of the microscope (excitation 550-580 nm, emission 600-650 nm). Scale bar is 20 μm.

2.3 Materials

3-methyl-4-nitrobenzoic acid, 4-methyl-3-nitrobenzoic acid, methyl 4-amino-2-methoxybenzoate,4-bromo-2-methylaniline,*N*-bromosuccinimide,paraformaldehyde,3-hydroxy-3-methyl-2-butanone, malononitrile, 4-methyl-2-nitroanisole, 4-methyl-3-nitrophenol, 2-*tert*-butylaniline, tetrabutylammonium tribromide, iodomethane, sodium phenoxide, sodium perborate tetrahydrate,copper(I) cyanide, [1,1'-Bis(diphenylphosphino)ferrocene]dichloropalladium ($Pd(dppf)Cl_2$), dimethylzinc solution (2.0 M in toluene), diisobutylaluminum hydride (DIBAL, 1.0 M in THF), manganese(IV) oxide, PBS (pH7.4, 10 mM),these chemicals were purchased from Sigma-Aldrich. All chemicals were used as received, without any further purification. Solvents for NMR analysis (Cambridge Isotope Laboratories) were used as received.

2.4 Methods

UV-vis absorption spectra were recorded on a Varian Cary 50 spectrophotometer. Fluorescence spectra were record on a Varian Cary Eclipse fluorescence spectrophotometer. ^{1}H NMR and ^{13}C NMR was acquired on Varian 300, 400 or 500MHz NMR spectrometer. ESI-MS was collected on Finnigan LCQ^{TM} DUO LC/MS spectrometer. HPLC analysis was performed on Agilent 1100 series HPLC system. Luminescence digital photographs were taken with a Nikon D3000 camera. Cell fluorescence images were acquired on Nikon eclipse Ti inverted epifluorescence microscope with a Nikon Lens Light C-HGFI 130 W lamp. Confocal imaging was done using a Zeiss LSM 710-META confocal microscope. The photolysis of various ONPEs was carried out by exposure of ONPEs solution (methanol/PBS, 3:1 v/v) to a UV-lamp with 254 nm irradiation (3 $mW \cdot cm^{-2}$).

2.5 Synthesis

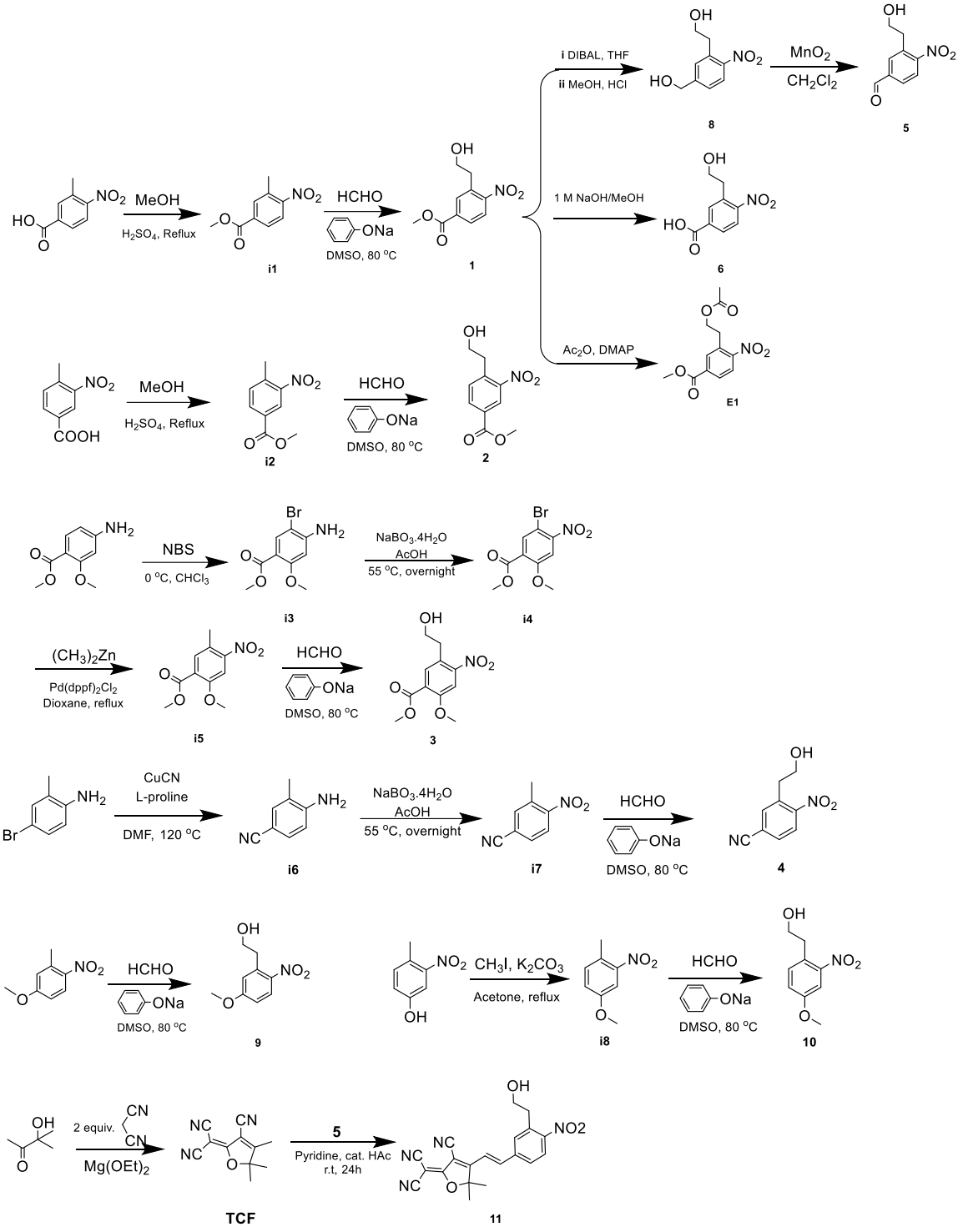

Scheme 2.3 Synthesis of ONPE compounds **1-11**.

Synthesis of ONPE 1

Methyl 3-methyl-4-nitrobenzoate (i1). To a solution of 3-methyl-4-nitrobenzoic acid (10 g, 55 mmol) in 100 mL methanol, concentrated H_2SO_4 (2 mL) was added dropwise and the solution was refluxed for 4 h. After cooling to room temperature, the solution was concentrated to 10 mL under vacuum, and was diluted with water (100 mL) and extracted with EtOAc (3×100 mL). The organic layer was washed with saturated $NaHCO_3$ and brine (100 mL each), dried over $MgSO_4$, filtered and concentrated to obtain **i1** as a pale yellow solid (96%).

^{1}H-NMR (300 MHz, $CDCl_3$): δ8.03 (m, 1H), 7.97 (m, 2H), 3.96 (s, 3H), 2.62 (s, 3H) ppm.

Methyl 3-(2-hydroxyethyl)-4-nitrobenzoate (1)[83]. To a solution of **i1** (2.92 g, 15 mmol) in DMSO (8 mL) was added paraformaldehyde (0.31 g, 10 mmol) and sodium phenoxide (25 mg). After stirring at 80°C for 3 h in dark, the reaction was diluted with water (100 mL) and extracted with EtOAc (3×100 mL). The organic layer was dried over $MgSO_4$, filtered, and concentrated. The product was purified by flash chromatography on silica gel (EtOAc : DCM= 1 : 3, v/v) to obtained **1**as a light yellow solid (28%).

^{1}H NMR (300 MHz, $CDCl_3$): δ8.12 (d, J = 1.8 Hz, 1H), 8.03 (dd, J = 2.1, 8.4 Hz, 1H),7.51 (d, J = 8.1 Hz, 1H), 3.97 (m, 5H), 3.18 (t, J = 6 Hz, 2H) ppm.

^{13}C NMR (125 MHz, $CDCl_3$): δ165.44, 152.68, 134.16, 134.07, 133.93, 128.91, 124.91, 62.69, 52.99, 35.90 ppm.

Synthesis of ONPE 2

Methyl 4-methyl-3-nitrobenzoate (i2). To a solution of 4-methyl-3-nitrobenzoic acid (10 g, 55 mmol) in 100 mL methanol, concentrated H_2SO_4 (2 mL) was added dropwise and was refluxed for 4 h. After cooling to room temperature, the solution was concentrated to 10 mL under vacuum, and was diluted with water (100 mL) and extracted with EtOAc (3×100 mL). The organic layer

was washed with saturated $NaHCO_3$ and brine (100 mL each), dried over $MgSO_4$, filtered and concentrated to obtain **i2**as a pale yellow solid (95%).

^{1}H NMR (300 MHz, $CDCl_3$): δ 8.60 (d, J = 1.8 Hz, 1H), 8.14 (dd, J = 1.8, 8.1 Hz, 1H), 7.44 (dd, J = 0.6, 8.1 Hz, 1H), 3.96 (s, 3H), 2.66 (s, 3H) ppm.

Methyl 4-(2-hydroxyethyl)-3-nitrobenzoate (2).[83] To a solution of **i1** (3 g, 15 mmol) in DMSO (8 mL) was added paraformaldehyde (0.31 g, 10 mmol) and sodium phenoxide (25 mg). After stirring at 80°C for 3 h in dark, the reaction was diluted with water (100 mL) and extracted with EtOAc (3×100 mL). The organic layer was dried over $MgSO_4$, filtered, and concentrated. The product was purified by flash chromatography on silica gel (EtOAc : DCM= 1 : 3, v/v) to obtained **i1**as a light yellow solid. (24%)

^{1}H NMR (300 MHz, $CDCl_3$): δ 8.52 (d, J = 1.8 Hz, 1H), 8.16 (dd, J = 1.8, 8.1 Hz, 1H), 7.54 (d, J = 8.1 Hz), 3.96 (m, 5H), 3.20 (t, J = 6.3, 2H) ppm. (26%)

^{13}C NMR (75 MHz, $CDCl_3$): δ 165.03, 149.74, 138.75, 133.26, 133.15, 129.83, 125.84, 62.23, 52.71, 36.09 ppm.

Synthesis of ONPE 3

Methyl 4-amino-5-bromo-2-methoxybenzoate (i3). To a solution of methyl 4-amino-2-methoxybenzoate (1.81 g, 10 mmol) in 100 mL $CHCl_3$ at 0 °C was slowly added NBS (1.78g, 10 mmol) under stirring in 1 h. The reaction was stirred at 0 °C for another 30 min. Thereafter, water (100 mL) was added to quench the reaction. The organic shell was collected and washed with water (100 mL), dried over MgSO4, filtered and concentrated to obtain the crude compound, which was further purified via a flash column chromatography on silica gel using the indicated eluent (EtOAc : DCM= 1 : 4, v/v) to get the **i3** (73%).

^{1}H NMR (400 MHz, $CDCl_3$): δ7.98 (s, 1H), 6.29 (s, 1H), 4.49 (s, 2H), 3.85 (s, 3H), 3.83 (s, 3H) ppm.

Methyl 5-bromo-2-methoxy-4-nitrobenzoate (i4). To a solution of **i3** (1.04 g, 4 mmol) in acetic acid (50 mL) was added $NaBO_3 \cdot 4H_2O$ 3.07 g, 20 mmol) and was stirred at 55 °C for overnight. After cooling to room temperature, the solution was neutralized with saturated $NaHCO_3$. The resulting solution was extracted with EtOAc (3 × 50 mL) and the organic layer was dried over $MgSO_4$, filtered and concentrated. A flash column chromatography on silica gel using DCM as eluent afforded the purified product **i4** (52%).

^{1}H NMR (300 MHz, $CDCl_3$): δ8.10 (s, 1H), 7.42 (s, 1H), 3.96 (s, 3H), 3.93 (s, 3H) ppm.

Methyl 2-methoxy-5-methyl-4-nitrobenzoate (i5).[84] To a solution of **i4** (67 mg, 0.3 mmol) and Pd(dppf)Cl_2(3 mg) in dry dioxane (1 mL) was added 350 µL of dimethylzinc solution (2.0 M in toluene) under Ar. The mixture was refluxed in dark for 3 h and quenched by adding methanol (1 mL). The solution was diluted with 10 mL DCM, washed with HCl (1 mM), water and dried over MgSO4. The product was purified by flash chromatography on silica gel (DCM) to obtained **i5** (90%).

^{1}H NMR (300 MHz, $CDCl_3$): δ7.72 (s, 1H), 7.56 (s, 1H), 3.95 (s, 3H), 3.93 (s, 3H), 2.54 (s, 3H) ppm.

Methyl 5-(2-hydroxyethyl)-2-methoxy-4-nitrobenzoate (3)[83].To a solution of **i5** (60 mg, 15 mmol) in DMSO (8 mL) was added paraformaldehyde (0.31 g, 10 mmol) and sodium phenoxide (25 mg). After stirring at 80°C for 3 h in dark, the reaction was diluted with water (100 mL) and extracted with EtOAc (3 × 100 mL). The organic layer was dried over $MgSO_4$, filtered, and concentrated. The product was purified by flash chromatography on silica gel (EtOAc : DCM= 1 : 3, v/v) to obtained **i1**(23%).

^{1}H NMR (300 MHz, $CDCl_3$): δ7.81 (s, 1H), 7.50 (s, 1H), 3.95 (m, 8H), 3.11 (t, J = 5.4 Hz, 2H) ppm.

Synthesis of ONPE 4

4-amino-3-methylbenzonitrile (i6).[85] To a solution of 4-bromo-2-methylaniline (500 mg, 2.7 mmol) in DMF (3 mL) was added CuCN (480 mg, 5.4 mmol) and L-proline (115 mg, 1 mmol). The reaction mixture was stirred under argonat 120 °C for 24 h. After cooling to room temperature, the reaction mixture was diluted with EtOAc (30 mL) and washed with water (3 × 10 mL). The organic layer was dried over $MgSO_4$, filtered and concentrated. A flash column chromatography on silica gel using the indicated eluent (EtOAc : hexane = 1 : 2, v/v) afforded the purified product**i6** as a purple solid. (33%)

^{1}H NMR (500 MHz, $CDCl_3$):δ7.31 (m, 1H), 6.63 (d, J = 8.5 Hz, 1H), 4.08 (s, 2H), 2.15 (s, 3H) ppm.

^{13}C NMR (125 MHz, $CDCl_3$): δ151.71, 136.71, 134.86, 130.92, 125.47, 117.10, 116.85, 20.13 ppm.

3-methyl-4-nitrobenzonitrile (i7).To a solution of **i6** (30 mg, 0.227 mmol) in acetic acid (3 mL) was added $NaBO_3 \cdot 4H_2O$ (0.21 g, 1.36 mmol) and was stirred at 55 °C overnight. After cooling to room temperature, the reaction was quenched with water (10 mL) and the solution was neutralized with saturated $NaHCO_3$. The resulting solution was extracted with EtOAc (3 × 100 mL) and the organic layer was dried over $MgSO_4$, filtered, concentrated, and purified via flash column chromatography on silica gel using the indicated eluent (EtOAc : hexane = 1 : 2, v/v) afforded **i7** as an orange solid (67%).

^{1}H NMR (500 MHz, $CDCl_3$): δ8.00 (d, J = 8.5 Hz, 1H), 7.65-7.68 (m, 2H), 2.62 (s, 6H) ppm.

^{13}C NMR (125 MHz, $CDCl_3$): δ 148.92, 134.42, 131.82, 122.26, 120.46, 114.44, 100.53, 17.23 ppm.

3-(2-hydroxyethyl)-4-nitrobenzonitrile (4)[83]. To a solution of **i7** (31 mg, 0.19 mmol) in DMSO (1 mL) was added paraformaldehyde (3.6 mg, 0.12 mmol) and sodium phenoxide (1 mg). After stirring at 80 °C for 3 h in dark, the reaction was diluted with water (15 mL) and extracted with EtOAc (3 × 20 mL). Combined organic layer was dried over $MgSO_4$ and concentrated. A flash column chromatography on silica gel (EtOAc : hexane = 1:2, v/v) was used to purify the product to obtain **4** as a yellow solid (30%).

^{1}H NMR (500 MHz, $CDCl_3$):δ 7.96 (d, *J* =8.5 Hz, 1H), 7.79 (d, *J* = 1.5 Hz, 1H), 7.70 (dd, *J* = 1.5, 8.5 Hz, 1H), 3.97 (t, *J* = 6.0 Hz, 3H), 3.17 (t, *J* = 6.0 Hz 3H) ppm.

^{13}C NMR (125 MHz, $CDCl_3$): δ 152.34, 136.90, 135.48, 131.37, 125.46, 117.09, 116.72, 62.11, 35.43 ppm.

Synthesis of ONPEs 5, 6 and 8

2-(5-(hydroxymethyl)-2-nitrophenyl)ethan-1-ol (8).[86]A solution of**1** (0.53 g, 0.37 mmol) in anhydrous THF (2 mL) at 0 °C was added 5 mL of DIBAL (1.0 M in THF) dropwise under argon. After stirring at 0 °C for 30 min, the reaction was warm to room temperature and stirred for another 3 h in dark. Thereafter, the reaction was quenched with methanol (10 mL), diluted with HCl (0.1M, 50 mL), and extracted with EtOAc (3×100 mL). Combined organic layer was dried over Na_2SO_4, filtered and concentrated. Purification by flash column chromatography on silica gel (EtOAc : DCM = 3:1, v/v) gave **8** as an orange solid (66%).

^{1}H NMR (300 MHz, $CDCl_3$):δ 7.97 (d, *J* = 8.1 Hz, 1H), 7.44 (s, 1H), 7.39 (d, *J* = 8.4 Hz, 1H), 4.80 (d, *J* = 5.1 Hz, 2H), 3.98 (dd, *J* = 3.3, 11.4 Hz, 2H), 3.21 (t, *J* = 6.6 Hz, 2H) ppm.

3-(2-hydroxyethyl)-4-nitrobenzaldehyde (5). To a solution of **8** (100 mg, 0.51 mmol) in anhydrous DCM (3 mL) was added MnO_2 (227 mg, 2.61 mmol). The reaction mixture was stirred at room temperature overnight in dark. Thereafter, the reaction was diluted with EtOAc (20 mL), and filtered through celite to remove the MnO_2. The solution was concentrated and the crude compound was purified *via* a flash column chromatography on silica gel (EtOAc : DCM = 1 : 3, v/v) to give **5** (78%).

^{1}H NMR (500 MHz, $CDCl_3$):δ 10.1 (s, 1H), 8.00 (d, J = 8.5 Hz, 1H), 7.96 (s, 1H), 7.89 (d, J = 8.5 Hz, 1H), 3.99 (t, J = 5.0 Hz, 2H), 3.21 (t, J = 5.0 Hz, 2H) ppm.

^{13}C NMR (125 MHz, $CDCl_3$):δ 190.63, 153.41, 138.66, 134.20, 128.48, 125.52, 62.47, 35.72 ppm.

3-(2-hydroxyethyl)-4-nitrobenzoic acid (6).To a solution of **1** (0.45 g, 2 mmol) in methanol (10 mL) was added 0.5 mL of NaOH aqueous solution (1 M). The reaction mixture was stirred at room temperature for 3 h. Thereafter, the reaction was diluted with water (20 mL), and the pH was adjusted to 2.0 using HCl (1 M). The solution was extracted with EtOAc (3 × 100 mL) and concentrated in vacuum to afford **6**. (90%)

^{1}H NMR (300 MHz, DMSO-d_6):δ13.52 (br, 1H), 8.06 (s, 1H), 7.97 (s, 2H), 4.77 (s, 1H), 3.64 (s, 2H), 3.01 (t, J = 6.0 Hz, 2H) ppm.

^{13}C NMR (75 MHz, DMSO-d_6):δ 166.38, 153.51, 134.57, 134.44, 133.91, 128.72, 124.79, 61.14, 35.27 ppm.

Synthesis of ONPE 9

2-(5-methoxy-2-nitrophenyl)ethanol (9).[83]To a solution of 4-methyl-2-nitroanisole (2.50 g, 15 mmol) in DMSO (8 mL) was added paraformaldehyde (0.31 g, 10 mmol) and sodium phenoxide (25 mg). After stirring at 80°C for 3 h in dark, the reaction was diluted with water (100 mL) and extracted with EtOAc (3×100 mL). The organic layer was dried over $MgSO_4$, filtered, and

concentrated. The product was purified by flash chromatography on silica gel (EtOAc : DCM= 1: 1, v/v) to obtained **9** as a light yellow solid (19%).

^{1}H NMR (400 MHz, $CDCl_3$): δ7.99 (d, J = 0.8 Hz, 1H), 6.87 (d, J = 2.8 Hz, 1H), 6.81 (dd, J = 2.8, 9.2 Hz, 1H), 3.87 (s, 5H), 3.36 (s, 1H), 3.17 (t, J = 6.4 Hz, 2H) ppm.

^{13}C NMR (100 MHz, $CDCl_3$): δ 163.23, 142.36, 137.45, 127.92, 117.96, 112.48, 62.44, 55.91, 37.23 ppm.

Synthesis of ONPE 10

4-methoxy-1-methyl-2-nitrobenzene (i8).To a solution of 4-methyl-3-nitrophenol (3.06 g, 20 mmol) in acetone (50 mL) was added iodomethane (3 mL) and potassium carbonate (2.0 g). The mixture was refluxed overnight. After cooling to room temperature, the reaction was diluted with water (100 mL) and extracted with DCM (2×100 mL). The organic layer was washed with saturated $NaHCO_3$and dried over $MgSO_4$, filtered, and concentrated to obtained **i8**without further purification (91%).

^{1}H NMR (300 MHz, $CDCl_3$):δ7.40 (d,J = 2.7 Hz, 1H), 7.16 (d,J = 8.7 Hz, 1H), 7.00 (dd, J = 3, 8.4 Hz, 1H), 3.80 (s, 3H), 2.45 (s, 3H)ppm.

2-(4-methoxy-2-nitrophenyl)ethanol (10).[83] To a solution of **i8**(2.50 g, 15 mmol) in DMSO (8 mL) was added paraformaldehyde (0.31 g, 10 mmol) and sodium phenoxide (25 mg). After stirring at 80°Cfor 3 h in dark, the reaction was diluted with water (100 mL) and extracted with EtOAc (3×100 mL). The organic layer was dried over $MgSO_4$, filtered, and concentrated. The product was purified by flash chromatography on silica gel (EtOAc : DCM= 1: 1, v/v) to obtained **10** (22%).

^{1}H NMR (300 MHz, $CDCl_3$):δ7.41 (d, J = 2.7 Hz, 1H), 7.30 (d, J = 8.7 Hz, 1H), 7.08 (dd, J = 2.8, 8.7 Hz, 1H), 3.87-3.84 (br, 5H), 3.06 (t, J = 6.6 Hz, 2H), 2.52. (s, 1H) ppm.

^{13}C NMR (75 MHz, $CDCl_3$):δ158.48, 149.97, 133.61, 125.64, 119.70, 109.40, 62.66, 55.80, 53.46 ppm.

Synthesis of TCF-ONPE derivative 11

2-(3-cyano-4,5,5-trimethylfuran-2(5H)-ylidene)malononitrile (TCF).The TCF was synthesized *via* a reported approach[87]. Briefly, to a solution of 3-hydroxy-3-methyl-2-butanone (1.0 g, 10 mmol) in absolute ethanol was added malononitrile (1.33 g, 20 mmol) and lithium (1 mg). The solution was stirred at 75 °C overnight in dark. After cooling to room temperature, the solution was concentrated. The residue was collected and washed by water, and was recrystallized from ethanol to obtain **TCF** (87%).

^{1}H NMR (300 MHz, $CDCl_3$): δ2.38 (s, 3H), 1.65 (s, 6H) ppm.

(E)-2-(3-cyano-4-(3-(2-hydroxyethyl)-4-nitrostyryl)-5,5-dimethylfuran-2(5H)-ylidene)malononitrile (11). A solution of **5** (25.4 mg, 0.130 mmol) and **TCF** (38.6 mg, 0.194 mmol) in pyridine (2 mL) was added drops of acetic acid. The mixture was stirred at 40 °C in dark overnight. Thereafter, the reaction mixture was concentrated and was diluted with EtOAc (50 mL). The organic layer was washed with diluted HCl (0.1M, 100 mL) and water (100 mL), dried over $MgSO_4$ and concentrated. Flash column chromatography on silica gel (EtOAc : hexane = 1: 1, v/v) was used to purify the product. Compound **11** was obtained as an orange solid (15%).

^{1}H NMR (500 MHz, DMSO): δ8.00-8.04 (m, 3H), 7.91 (d, J = 16.5 Hz, 1H), 7.37 (d, J = 17 Hz, 1H), 3.66 (t, J = 6.0 Hz, 2H), 3.04 (t, J = 6.0 Hz, 2H), 1.813 (s, 3H), 1.810 (s, 3H) ppm.

^{13}C NMR (125 MHz, DMSO):δ176.8, 174.0, 150.7, 144.1, 138.1, 133.3, 127.7, 124.8, 118.4, 112.4, 111.5, 110.4, 101.5, 99.5, 60.7, 55.2, 35.0, 28.9, 24.9 ppm.

MS (ESI): Calculated 376.1, found 375.1 $[M-H]^-$.

Synthesis of C1

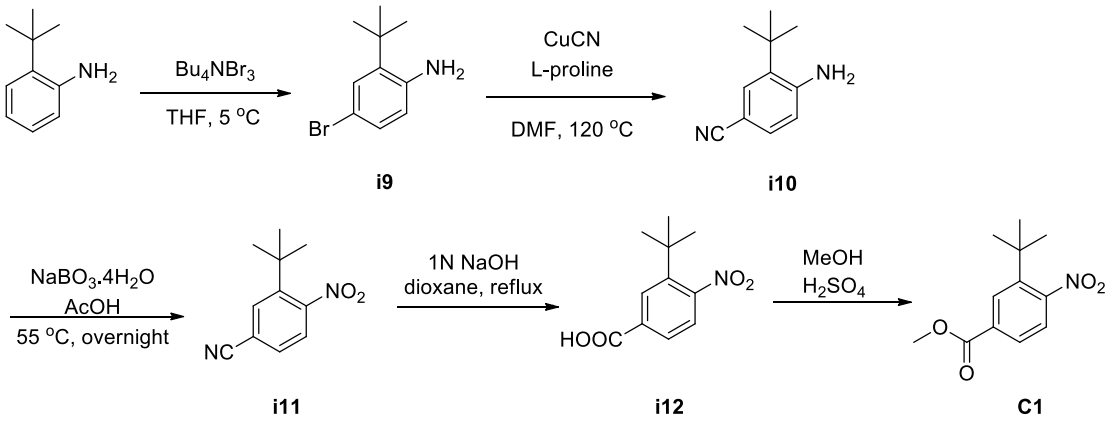

Scheme 2.2 synthesis of reference compound **C1**

4-bromo-2-(*tert*-butyl)aniline (i9). To a solution of 2-*tert*-butylaniline (1.49 g, 10 mmol) in THF (20 mL) at 5 °C was added a solution of tetrabutylammonium tribromide (4.38 g, 9.1 mmol) in THF (3 mL) dropwisely. After stirring at 4 °C or 30 min, the reaction was quenched with water (10 mL). The mixture was diluted with diethyl ether (200 mL) and washed with saturated $NaHCO_3$ solution (200 mL) and brine (200 mL). Resulting solution was dried over Na_2SO_4, filtered and concentrated to give **i9** as brown oil (98%).

^{1}H NMR (300 MHz, $CDCl_3$): δ7.32 (d, J = 2.4 Hz, 1H), 7.12 (dd, J = 2.4, 8.4 Hz, 1H), 6.56 (d, J = 8.4 Hz, 1H), 4.11 (s, 2H), 1.40 (s, 9H) ppm.

4-amino-3-(*tert*-butyl)benzonitrile (i10). A solution of CuCN (179 mg, 2 mmol), L-proline (115 mg, 1 mmol) and**i9** (228 mg, 1 mmol) in DMF (3 mL) was stirred at 120 °Cunder argon for 2 days. After cooling to room temperature, the reaction mixture was diluted with EtOAc (15 mL) and washed with water (3 × 10 mL). The organic layer was dried over Na_2SO_4 filtered and concentrated. A flash column chromatography on silica gel using the indicated eluent (EtOAc : hexane = 1 : 2, v/v) afforded the **i10**(47%).

^{1}H NMR (300 MHz, $CDCl_3$):δ 7.47 (d, J = 1.8 Hz, 1H), 7.29 (dd, J = 1.8, 8.4 Hz, 1H), 6.61 (d, J = 8.4 Hz, 1H), 4.11 (s, 2H), 1.40 (s, 9H) ppm.

3-(*tert*-butyl)-4-nitrobenzonitrile (i11). The solution of **i10** (81.3 mg, 0.47 mmol) and $NaBO_3 \cdot 4H_2O$ (431 mg, 2.8 mmol) in acetic acid (5 mL) was stirred at 55 °C overnight. After cooling to room temperature, the reaction was quenched with water (10 mL), and neutralized with saturated $NaHCO_3$ solution, and extracted with EtOAc (3 × 100 mL). Combined organic layer was dried over $MgSO_4$, filtered and concentrated. A flash column chromatography on silica gel using the indicated eluent (EtOAc : hexane = 1 : 2, v/v) afforded the purified product **i11** as an orange solid (66%).

^{1}H NMR (500 MHz, $CDCl_3$):δ 7.87 (d, *J* = 2.0 Hz, 1H), 7.62 (dd, *J* = 2.0, 8.5 Hz, 1H), 7.41 (d, *J* = 8.5 Hz, 1H), 1.42 (s, 9H) ppm.

3-(*tert*-butyl)-4-nitrobenzoic acid (i12).A mixture of **i11** (63 mg, 0.31 mmol) in 1,4-dioxane (2 mL) and 1 mL of NaOH aqueous solution (1 M) was refluxed overnight. After cooling to room temperature, the mixture was diluted with water (10 mL) and the pH of the solution was adjusted to 1 using HCl solution (1M). The resulting solution was extracted with EtOAc (3×100 mL). Combined organic layer was washed with brine (100 mL), dried over $NaSO_4$, filtered and concentrated to get product **i12**(82%).

^{1}H NMR (500 MHz, $CDCl_3$):δ 8.33 (d, *J* = 1.8 Hz, 1H), 8.00 (dd, *J* = 1.8, 8.1 Hz, 1H), 7.40 (d, J = 8.1 Hz, 1H), 1.45 (s, 9H) ppm.

Methyl 3-(tert-butyl)-4-nitrobenzoate (C1). A solution of **i12** (57 mg, 0.26 mmol) in methanol (5 mL) was added few drops of concentrated H_2SO_4 and was refluxed for 5 h. After cooling to room temperature, the reaction mixture was diluted with water (50 mL) and extracted with EtOAc (2 × 50 mL). The organic layer was washed with saturated $NaHCO_3$and dried over $NaSO_4$, filtered and concentrated to get **C1** as a pale yellow solid. (98%)

^{1}H NMR (500 MHz, $CDCl_3$):δ 8.24 (d, *J*= 2.0 Hz, 1H), 7.93 (dd, *J* = 2.0, 8.0 Hz, 1H), 7.34 (d, *J* = 8.0 Hz, 1H), 3.94 (s, 3H), 1.41 (s, 9H) ppm.

^{13}C NMR (125 MHz, $CDCl_3$): δ 165.6, 153.5, 141.8, 132.2, 130.6, 128.4, 124.2, 52.8, 36.1, 30.8 ppm.

Synthesis of E1

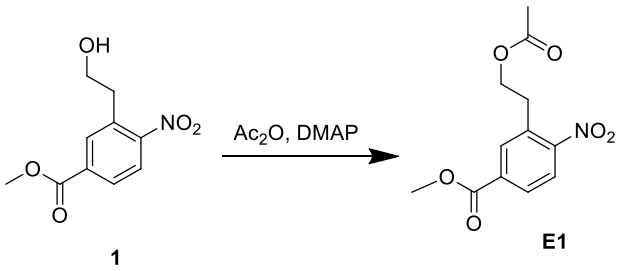

Scheme 2.3 Synthesis of **E1**

To a solution of **1** (0.45 g, 2 mmol) and 10 mg of DMAP in $CHCl_3$ (10 mL) at 0 °C was added 1 mL of acetic anhydride. The reaction mixture was stirred 0 °C for 30 min and recovered to room temperature for 3 h. Thereafter, the reaction was diluted with water (20 mL), extracted with EtOAc (3 × 100 mL) and washed with brine. The organic layer was dried over Na_2SO_4 and concentrated in vacuum to afford **E1,** no further purification required. (93%)

^{1}H NMR (300 MHz, $CDCl_3$): δ 7.99 (d, *J*= 1.6 Hz, 2H), 7.90 (d, *J* = 8.1 Hz, 1H), 4.33 (t, *J* = 6.3 Hz, 1H), 3.94 (s, 3H), 3.24 (t, *J* = 6.3 Hz, 1H), 1.98 (s, 3H) ppm.

^{13}C NMR (75 MHz, $CDCl_3$): δ 170.69, 165.02, 152.32, 133.76, 133.01, 128.94, 124.75, 63.47, 52.74, 31.95, 20.72 ppm.

Chapter 3

Conclusion and Perspective

Photoactivatable fluorophores have generated a variety of important applications in biological research. The development of photoactivatable fluorophores has been largely put on modify the fluorescence profile and biocompatibility of the organic dyes and the improvement of uncaging efficiency. The ONPE based fluorophores I presented here are a new class of photoactivatable fluorophores manifesting a number of desired properties for in vitro imaging. These fluorophores are self-caged that only generate water as byproduct during uncaging process. This circumvent the problem of cytotoxic byproducts generation suffered in many *o*-nitrobenzyl based PPGs. The structure relationship was carefully tested. In order to get a bathochromic shift of absorption and emission bands and large fluorescence enhancement, we found that strong EWGs are preferred in the 5-position of phenyl ring. In the case of 5-methylcarbonyl group, the fluorescence turn on/off ratio can reach up to 800 fold. A mechanism involves the keto-enol tautomerizaion was proposed to rationale the fluorescence enhancement mechanism of ONPE fluorophores. Based on our findings, we successfully synthesized TCF-ONPE (**11**) and demonstrated its application as an excellent biomarker.

The development of ONPE fluorophores provides a new strategy to design photoactivatable fluorescent probes. The next stage of ONPE based fluorophores should focus on the following points. First, improve the photostability of ONPE dyes. Second, further modify the fluorescence profile of ONPE dyes. For bioapplication, the ideal absorption should go beyond visible range. Third, constructing fluorescent probes for specific biochemical problems, for instance, designing specific-targeting fluorescence labels to track the interactions of subcell organelles or proteins. Using some well-established bioorthogonal organic reactions[88] such as thiol-ene reaction[89], Staudinger reaction[90,91] or Diels-Alder reaction[92] to conjugate the probe to proteins of interest could a good way to construct fluorescent probe of ONPE fluorophores.

Overall, this ONPE based photoactivatable fluorophore have a bright future as a versatile and powerful tool for fluorescent biolabeling.

References

(1) Valeur, B.; Berberan-Santos, M. N. *J. Chem. Educ.* **2011**, *88*, 731.
(2) Stokes, G. G. *Philosophical Transactions of the Royal Society of London* **1852**, *142*, 463.
(3) Strickler, S. J.; Berg, R. A. *The Journal of Chemical Physics* **1962**, *37*, 814.
(4) Berezin, M. Y.; Achilefu, S. *Chem. Rev.* **2010**, *110*, 2641.
(5) Bates, M.; Huang, B.; Dempsey, G. T.; Zhuang, X. *Science* **2007**, *317*, 1749.
(6) Rust, M. J.; Bates, M.; Zhuang, X. *Nature methods* **2006**, *3*, 793.
(7) Belov, V. N.; Wurm, C. A.; Boyarskiy, V. P.; Jakobs, S.; Hell, S. W. *Angew. Chem. Int. Ed.* **2010**, *49*, 3520.
(8) BETZIG, E.; TRAUTMAN, J. K.; HARRIS, T. D.; WEINER, J. S.; KOSTELAK, R. L. *Science* **1991**, *251*, 1468.
(9) Lukyanov, K. A.; Chudakov, D. M.; Lukyanov, S.; Verkhusha, V. V. *Nat Rev Mol Cell Biol* **2005**, *6*, 885.
(10) Lippincott-Schwartz, J.; Patterson, G. H. In *Methods in Cell Biology*; Academic Press: 2008; Vol. Volume 85, p 45.
(11) Shimomura, O.; Johnson, F. H.; Saiga, Y. *Journal of Cellular and Comparative Physiology* **1962**, *59*, 223.
(12) Prasher, D. C.; Eckenrode, V. K.; Ward, W. W.; Prendergast, F. G.; Cormier, M. J. *Gene* **1992**, *111*, 229.
(13) Chalfie, M.; Tu, Y.; Euskirchen, G.; Ward, W.; Prasher, D. *Science* **1994**, *263*, 802.
(14) Inouye, S.; Tsuji, F. I. *FEBS Lett.* **1994**, *341*, 277.
(15) Tsien, R. Y. *Annu. Rev. Biochem* **1998**, *67*, 509.
(16) Chalfie, M. *Photochem. Photobiol.* **1995**, *62*, 651.
(17) Mitra, R. D.; Silva, C. M.; Youvan, D. C. *Gene* **1996**, *173*, 13.
(18) Shaner, N. C.; Campbell, R. E.; Steinbach, P. A.; Giepmans, B. N. G.; Palmer, A. E.; Tsien, R. Y. *Nat Biotech* **2004**, *22*, 1567.
(19) Rizzo, M. A.; Springer, G. H.; Granada, B.; Piston, D. W. *Nat Biotech* **2004**, *22*, 445.
(20) Bao, G.; Mitragotri, S.; Tong, S. *Annual Review of Biomedical Engineering* **2013**, *15*, 253.
(21) Subramaniam, P.; Lee, S. J.; Shah, S.; Patel, S.; Starovoytov, V.; Lee, K.-B. *Adv. Mater.* **2012**, *24*, 4014.
(22) Page Faulk, W.; Malcolm Taylor, G. *Immunochemistry* **1971**, *8*, 1081.
(23) Elghanian, R.; Storhoff, J. J.; Mucic, R. C.; Letsinger, R. L.; Mirkin, C. A. *Science* **1997**, *277*, 1078.
(24) Oldenburg, S. J.; Averitt, R. D.; Westcott, S. L.; Halas, N. J. *Chem. Phys. Lett.* **1998**, *288*, 243.
(25) Smith, A. M.; Dave, S.; Nie, S.; True, L.; Gao, X. *Expert Review of Molecular Diagnostics* **2006**, *6*, 231.
(26) Han, G.; Mokari, T.; Ajo-Franklin, C.; Cohen, B. E. *J. Am. Chem. Soc.* **2008**, *130*, 15811.
(27) Kim, S.; Lim, Y. T.; Soltesz, E. G.; De Grand, A. M.; Lee, J.; Nakayama, A.; Parker, J. A.; Mihaljevic, T.; Laurence, R. G.; Dor, D. M.; Cohn, L. H.; Bawendi, M. G.; Frangioni, J. V. *Nat Biotech* **2004**, *22*, 93.
(28) Resch-Genger, U.; Grabolle, M.; Cavaliere-Jaricot, S.; Nitschke, R.; Nann, T. *Nat Meth* **2008**, *5*, 763.
(29) Michalet, X.; Pinaud, F. F.; Bentolila, L. A.; Tsay, J. M.; Doose, S.; Li, J. J.; Sundaresan, G.; Wu, A. M.; Gambhir, S. S.; Weiss, S. *Science* **2005**, *307*, 538.
(30) Shan, J.; Yong, Z.; Kian Meng, L.; Eugene, K. W. S.; Lei, Y. *Nanotechnology* **2009**, *20*, 155101.
(31) Wang, M.; Mi, C.-C.; Wang, W.-X.; Liu, C.-H.; Wu, Y.-F.; Xu, Z.-R.; Mao, C.-B.; Xu, S.-K. *ACS Nano* **2009**, *3*, 1580.

(32) Auzel, F. *Comptes Rendus Hebdomadaires Des Seances De L Academie Des Sciences Serie B* **1966**, *263*, 819.
(33) Ramasamy, P.; Manivasakan, P.; Kim, J. *RSC Advances* **2014**, *4*, 34873.
(34) van der Ende, B. M.; Aarts, L.; Meijerink, A. *PCCP* **2009**, *11*, 11081.
(35) Zou, W.; Visser, C.; Maduro, J. A.; Pshenichnikov, M. S.; Hummelen, J. C. *Nature Photonics* **2012**, *6*, 560.
(36) Xie, X.; Liu, X. *Nat Mater* **2012**, *11*, 842.
(37) Lai, J.; Shah, B. P.; Garfunkel, E.; Lee, K.-B. *ACS nano* **2013**, *7*, 2741.
(38) Li, Z.; Zhang, Y.; Jiang, S. *Adv. Mater.* **2008**, *20*, 4765.
(39) Dempsey, G. T.; Bates, M.; Kowtoniuk, W. E.; Liu, D. R.; Tsien, R. Y.; Zhuang, X. *J. Am. Chem. Soc.* **2009**, *131*, 18192.
(40) Klán, P.; Šolomek, T.; Bochet, C. G.; Blanc, A.; Givens, R.; Rubina, M.; Popik, V.; Kostikov, A.; Wirz, J. *Chem. Rev.* **2013**, *113*, 119.
(41) Schmierer, T.; Laimgruber, S.; Haiser, K.; Kiewisch, K.; Neugebauer, J.; Gilch, P. *PCCP* **2010**, *12*, 15653.
(42) Silva, C. R.; Reilly, J. P. *The Journal of Physical Chemistry* **1996**, *100*, 17111.
(43) Fang, W.-H.; Phillips, D. L. *ChemPhysChem* **2002**, *3*, 889.
(44) Schrock, A. K.; Schuster, G. B. *J. Am. Chem. Soc.* **1984**, *106*, 5228.
(45) Dockter, M. E. *J. Biol. Chem.* **1979**, *254*, 2161.
(46) Lord, S. J.; Conley, N. R.; Lee, H.-l. D.; Samuel, R.; Liu, N.; Twieg, R. J.; Moerner, W. *J. Am. Chem. Soc.* **2008**, *130*, 9204.
(47) Lord, S. J.; Conley, N. R.; Lee, H.-l. D.; Nishimura, S. Y.; Pomerantz, A. K.; Willets, K. A.; Lu, Z.; Wang, H.; Liu, N.; Samuel, R.; Weber, R.; Semyonov, A.; He, M.; Twieg, R. J.; Moerner, W. E. *ChemPhysChem* **2009**, *10*, 55.
(48) Lee, M. K.; Rai, P.; Williams, J.; Twieg, R. J.; Moerner, W. E. *J. Am. Chem. Soc.* **2014**, *136*, 14003.
(49) Lee, H.-l. D.; Lord, S. J.; Iwanaga, S.; Zhan, K.; Xie, H.; Williams, J. C.; Wang, H.; Bowman, G. R.; Goley, E. D.; Shapiro, L.; Twieg, R. J.; Rao, J.; Moerner, W. E. *J. Am. Chem. Soc.* **2010**, *132*, 15099.
(50) Yu, Z.; Ho, L. Y.; Lin, Q. *J. Am. Chem. Soc.* **2011**, *133*, 11912.
(51) Los, G. V.; Encell, L. P.; McDougall, M. G.; Hartzell, D. D.; Karassina, N.; Zimprich, C.; Wood, M. G.; Learish, R.; Ohana, R. F.; Urh, M. *ACS chemical biology* **2008**, *3*, 373.
(52) Crivat, G.; Taraska, J. W. *Trends Biotechnol.* **2012**, *30*, 8.
(53) v. Pechmann, H. *Berichte der deutschen chemischen Gesellschaft* **1884**, *17*, 929.
(54) Zheng, G.; Guo, Y.-M.; Li, W.-H. *J. Am. Chem. Soc.* **2007**, *129*, 10616.
(55) Sun, W.-C.; Gee, K. R.; Klaubert, D. H.; Haugland, R. P. *The Journal of Organic Chemistry* **1997**, *62*, 6469.
(56) Fülöp, L.; Penke, B.; Zarándi, M. *J. Pept. Sci.* **2001**, *7*, 397.
(57) Griffin, B. A.; Adams, S. R.; Tsien, R. Y. *Science* **1998**, *281*, 269.
(58) Mason, S. J.; Hake, J. L.; Nairne, J.; Cummins, W. J.; Balasubramanian, S. *The Journal of Organic Chemistry* **2005**, *70*, 2939.
(59) Zhuang, X. *Nat Photon* **2009**, *3*, 365.
(60) Gorka, A. P.; Nani, R. R.; Zhu, J.; Mackem, S.; Schnermann, M. J. *J. Am. Chem. Soc.* **2014**.
(61) Fernandez-Suarez, M.; Ting, A. Y. *Nat Rev Mol Cell Biol* **2008**, *9*, 929.
(62) Hell, S. W. *Science* **2007**, *316*, 1153.
(63) Kaur, G.; Costa, M. W.; Nefzger, C. M.; Silva, J.; Fierro-González, J. C.; Polo, J. M.; Bell, T. D. M.; Plachta, N. *Nat Commun* **2013**, *4*, 1637.
(64) Kobayashi, T.; Urano, Y.; Kamiya, M.; Ueno, T.; Kojima, H.; Nagano, T. *J Am Chem Soc* **2007**, *129*, 6696.

(65) Zhao, Y. R.; Zheng, Q.; Dakin, K.; Xu, K.; Martinez, M. L.; Li, W. H. *J Am Chem Soc* **2004**, *126*, 4653.
(66) Zheng, G. H.; Guo, Y. M.; Li, W. H. *J Am Chem Soc* **2007**, *129*, 10616.
(67) Warther, D.; Bolze, F.; Leonard, J.; Gug, S.; Specht, A.; Puliti, D.; Sun, X. H.; Kessler, P.; Lutz, Y.; Vonesch, J. L.; Winsor, B.; Nicoud, J. F.; Goeldner, M. *J Am Chem Soc* **2010**, *132*, 2585.
(68) Belov, V. N.; Wurm, C. A.; Boyarskiy, V. P.; Jakobs, S.; Hell, S. W. *Angew Chem Int Edit* **2010**, *49*, 3520.
(69) Maurel, D.; Banala, S.; Laroche, T.; Johnsson, K. *Acs Chem Biol* **2010**, *5*, 507.
(70) Ragab, S. S.; Swaminathan, S.; Baker, J. D.; Raymo, F. M. *Phys Chem Chem Phys* **2013**, *15*, 14851.
(71) Zhu, M. Q.; Zhu, L. Y.; Han, J. J.; Wu, W. W.; Hurst, J. K.; Li, A. D. Q. *J Am Chem Soc* **2006**, *128*, 4303.
(72) Uno, S. N.; Kamiya, M.; Yoshihara, T.; Sugawara, K.; Okabe, K.; Tarhan, M. C.; Fujita, H.; Funatsu, T.; Okada, Y.; Tobita, S.; Urano, Y. *Nat Chem* **2014**, *6*, 681.
(73) Yu, Z. P.; Ho, L. Y.; Lin, Q. *J Am Chem Soc* **2011**, *133*, 11912.
(74) Klan, P.; Solomek, T.; Bochet, C. G.; Blanc, A.; Givens, R.; Rubina, M.; Popik, V.; Kostikov, A.; Wirz, J. *Chem Rev* **2013**, *113*, 119.
(75) Zhao, H.; Sterner, E. S.; Coughlin, E. B.; Theato, P. *Macromolecules* **2012**, *45*, 1723.
(76) Bochet, C. G. *J Chem Soc Perk T 1* **2002**, 125.
(77) Lai, J. P.; Xu, Y. Y.; Mu, X.; Wu, X. L.; Li, C.; Zheng, J. S.; Wu, C. L.; Chen, J. B.; Zhao, Y. B. *Chem Commun* **2011**, *47*, 3822.
(78) Specht, A.; Bolze, F.; Omran, Z.; Nicoud, J. F.; Goeldner, M. *Hfsp J* **2009**, *3*, 255.
(79) Han, J. Y.; Burgess, K. *Chem Rev* **2010**, *110*, 2709.
(80) Lakowicz, J. R. *Principles of fluorescence spectroscopy*; 3rd ed.; Springer: New York, 2006.
(81) Dopp, D. *Chem Commun* **1968**, 1284.
(82) Zhou, X. F.; Su, F. Y.; Tian, Y. Q.; Youngbull, C.; Johnson, R. H.; Meldrum, D. R. *J Am Chem Soc* **2011**, *133*, 18530.
(83) Costero, A. M.; Parra, M.; Gil, S.; Gotor, R.; Mancini, P. M. E.; Martinez-Manez, R.; Sancenon, F.; Royo, S. *Chemistry-an Asian Journal* **2010**, *5*, 1573.
(84) Herbert, J. M. *Tetrahedron Lett* **2004**, *45*, 817.
(85) Wang, D. P.; Kuang, L. P.; Li, Z. W.; Ding, K. *Synlett* **2008**, 69.
(86) Yoon, N. M.; Gyoung, Y. S. *J Org Chem* **1985**, *50*, 2443.
(87) Zhang, T.; Peng Guo, K.; Qiu, L.; Shen, Y. *Synth. Commun.* **2006**, *36*, 1367.
(88) Kolb, H. C.; Finn, M. G.; Sharpless, K. B. *Angew. Chem. Int. Ed.* **2001**, *40*, 2004.
(89) Arumugam, S.; Popik, V. V. *J. Am. Chem. Soc.* **2012**, *134*, 8408.
(90) Adzima, B. J.; Tao, Y.; Kloxin, C. J.; DeForest, C. A.; Anseth, K. S.; Bowman, C. N. *Nat Chem* **2011**, *3*, 256.
(91) Baskin, J. M.; Prescher, J. A.; Laughlin, S. T.; Agard, N. J.; Chang, P. V.; Miller, I. A.; Lo, A.; Codelli, J. A.; Bertozzi, C. R. *Proceedings of the National Academy of Sciences* **2007**, *104*, 16793.
(92) Arumugam, S.; Popik, V. V. *J. Am. Chem. Soc.* **2011**, *133*, 15730.